Mixed-valence compounds*

C. M. Varma

Bell Laboratories, Murray Hill, New Jersey 07974

In a number of rare-earth compounds, the atomic-like *f* levels and the wide *s–d* band coexist at the Fermi level. Such compounds are being referred to as mixed-valence compounds. These compounds have a variety of unique thermal and magnetic properties. In this article, we review some salient experimental results in such compounds and discuss a theoretical framework in which they may be understood. Special emphasis is given to the Samarium chalcogenides, on which extensive experimental results are available. The review is not meant to be a comprehensive survey of theoretical and experimental results. Rather it reflects the interests of the author. The hope is that the basic unresolved issues in the theory of mixed-valence compounds are pointed out so as to stimulate further experimental and theoretical work.

CONTENTS

I. INTRODUCTION

In the past few years a great deal of research has been done on the properties of rare-earth metals and their compounds. Here we shall discuss a subclass of these materials which are being referred to as *mixed-valence* or *mixed-configuration* compounds and sometimes as *fluctuating-valence* or *fluctuating-configuration* compounds. There are more than twenty such compounds and new ones are rapidly being discovered. Some actinide compounds as well as transition metal compounds may also belong in this category.

These mixed-valence compounds are metallic in the sense that the dc conductivity is of a magnitude characteristic of metals (albeit poor), and the reflectivity data yield a plasma edge of the order of a volt, indicating a substantial number of free carriers. What sets these compounds apart from other metals is that, near the Fermi energy, both the very heavy *f* electrons, which obey atomic spectral rules to a good approximation, and the much lighter *s* and *d* electrons are present.

This is an interim review of the properties of these materials. The aim here is to identify the special features and parameters that characterize the mixed-valence compounds and to discuss a framework in which the experimental results can best be understood. This will, it is hoped, put into focus the unresolved issues in the properties of these compounds and stimulate further experiments. The field of mixed-valence compounds, we believe, is still in its adolescence. In view of this, this article is in the nature of a status report rather than a comprehensive review. The choice of material discussed here has been governed by the interests of the author and there is no effort made towards completeness in either the substance of the article or the referencing. The author readily apologizes for the omissions. The article itself is an outgrowth of notes prepared for a talk given at the 1975 March Meeting of the American Physical Society (Varma, 1975). Other reviews dealing with mixed-valence compounds, which are more experimental in emphasis than the present article, have been given by Maple and Wohleben (1973) and by Jayaraman *et al.* (1975b). A brief theoretical discussion of these compounds has been presented by Mott (1974).

A. Organization of the paper

We discuss first of all the terms *mixed valence* and *fluctuating valence*, and present the fundamental (*a priori*) characteristics that make a compound mixed-valent. We also try here to put these compounds in their proper context in theory of solids. The ideas discussed in part B of the introduction are then made more concrete by considering in Sec. II a model Hamiltonian for these compounds and an approximate ground-state wave function. This wave function provides a value for the average valence and the mean-square fluctuations about it. On the basis of such stationary states, we briefly comment on the type of information different experiments can reveal and discuss the minimum possible theory necessary to characterize the mixed-valence phase (the more exotic possibilities are mentioned only in passing in Sec. IV. A). Also, a possible new mode brought about by the presence of electrons of very different effective masses is discussed in Sec. II. Section III is devoted to a brief review of some crucial experiments together with some interpretive discussion. The list of experiments discussed is given in the Table of Contents. In Sec. IV we take up the question of the transition from insulator to mixed-valence metal, observed in several compounds

---

*Based on a talk given at the Meeting of the American Physical Society at Denver, March 1975.

TABLE I. The rare-earth elements, their most common oxidation states, and the electronic configuration of the oxidation states.

Element	Oxidation states	Electronic configuration 2^+	3^+	4^+
La	3		$4f^0$	
Ce	3, 4		$4f^1$	$4f^0$
Pr	3, 4		$4f^2$	$4f^1$
Nd	3		$4f^3$	
Pm	3		$4f^4$	
Sm	2, 3	$4f^6$	$4f^5$	
Eu	2, 3	$4f^7$	$4f^6$	
Gd	3		$4f^7$	
Tb	3, 4		$4f^8$	$4f^7$
Dy	3		$4f^9$	
Ho	3		$4f^{10}$	
Er	3		$4f^{11}$	
Tm	2, 3	$4f^{13}$	$4f^{12}$	
Yb	2, 3	$4f^{14}$	$4f^{13}$	
Lu	3		$4f^{14}$	

and discussed in Sec. III. Special attention is paid to the correlations between the anomalous features in the phase diagram of some mixed-valence materials and their special heat and anomalous thermal expansion. Finally, in Sec. V, we conclude with some remarks on the unsettled theoretical questions and on some important experiments that need to be performed.

B. Mixed valence, fluctuating valence?

The labels *mixed valence* and *fluctuating valence* are somewhat mysterious. By properly elucidating in what sense these materials have mixed and/or fluctuating valence, we can hopefully understand some of the basic physics involved. Let us, for example, consider the compound SmS, which at pressures above about 6 kbar has "mixed valence." Sm has the outer electronic structure $4f^6 5d^0 6s^2$ and sulfur has $3s^2 3p^4$. (In Table I, we list the rare-earth elements and their electronic configurations.) The compound at atmospheric pressure is an ionic semiconductor, of rock salt structure, and is nominally $\mathrm{Sm}^{2+}\mathrm{S}^{2-}$. This is already interesting because only Sm and Eu among the rare earths occur as 2+ ions in most of their compounds, whereas the other rare earths occur most often as 3+. (Yb and Tm also occur sometimes as 2+ ions; see discussion at the end of this section.) This is because of the increasing importance of Hund's-rule coupling as we approach the middle of the rare-earth series. The final occupied f level is, however, not far below the d level even in Sm. (In Eu^{2+}, which has the largest Hund's-rule coupling, the $5d$ level is over an eV above the final occupied f state.) In compounds the d levels broaden into a band, hybridizing in the process with the $6s$ band, but the f levels are relatively unaffected (apart from a change in their absolute position). In fact, the neutron scattering results (Shapiro *et al.*, 1975) and infrared experiments (Nathan *et al.*, 1975) on crystal field excitons in SmS are understood by assuming the f-wave functions to be more or less atomic. The electronic structure of SmS in the semiconducting phase is thus as shown in Fig. 1. Under pressure the lower of the crystal field split d-bands broadens and moves down in energy relative to the f level and ultimately crosses it. This closing of the gap under pressure is seen directly in infrared experiments (Wachter, 1969; Kaldis and Wachter, 1972; Narayanamurti *et al.*, 1974). Near the pressure where the f–d gap goes to zero, a metal insulator transition occurs, as evidenced for example by a large (~10%) change in volume, a change in resistivity, and also the change in color from black to golden (Jayaraman *et al.*, 1970; Chatterjee *et al.*, 1972; Jayaraman *et al.*, 1974).

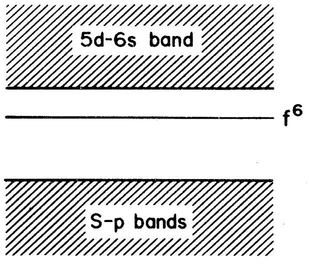

FIG. 1. Schematic electronic structure of samarium chalcogenides in the semiconducting phase.

In Fig. 3 a schematic electronic structure and density of states for the metallic phase is shown. The f levels now hybridize with the d level on a neighboring atom (they cannot hybridize with the d level on the same atom, since the f^6 configuration has a total $J=0$). The "bandwidth" of the hybridized f band can be estimated to be between 10^{-2} and 10^{-1} eV (Heine and Varma, 1974) so that in the density of states we have, over the smooth s–d background, a sharp peak attributable to f-like atomic character in a tight binding representation of the band. The wave functions near this peak are linear combinations of f-like and d-like wave functions:

$$\Psi_{\vec{k}} = a_{\vec{k}}\varphi_d + b_{\vec{k}}\varphi_f\,, \tag{I.1}$$

the proportion a_k to b_k varying rapidly near the peak. In Sec. II we shall discuss the derivation and properties of wave functions like (I.1) in detail. Here we note that since this peak is derived from the f^6 level which accommodates one electron per atom (correlation energy renders the f levels nondegenerate), the integrated density of states of f-like character in it is also one electron per atom. It follows therefore that the $T=0$ Fermi level is necessarily pinned to lie in the f peak. This is a simple but fundamental property of these materials and may be taken to define the mixed-valence compounds. The wave function (I.1) represents a linear combination of atomic orbital states which is partly $f^5 d$ and partly f^6. Now the d electron is relatively free and is not affected by the local atomic exchange and correlations nearly as much as the f electrons. So we might say that the wave function (I.1) represents a linear combination of 3+ and 2+ valence states on the rare-earth ion. It is only in this sense that these materials have mixed valence. A measure of the average valence may be defined from wave functions like (I.1) to be

$$R = \sum_{\vec{k}} |a_{\vec{k}}|^2 \Big/ \sum_{k} |b_{\vec{k}}|^2\,, \tag{I.2}$$

where we sum over the occupied part of the conduction band. The ratio R can thus be altered by moving the bottom of the d band with respect to the f levels by (a) applying pressure, (b) appropriate doping, or (c) changing the temperature. Because the *f* electrons have a nonzero bandwidth, the instantaneous valence in general will be different from (I.2). Large fluctuations involving states of more than one *f* electron at a site can be excluded due to the large Coulomb repulsion, but instantaneously the local *f* character can have fluctuations (calculated in Sec. II) around the value (I.2), the characteristic time scale of these fluctuations being determined by the *f* bandwidth. In this sense these compounds have a fluctuating valence.

One may ask, what is the difference between this situation and transition metals and transition metal compounds, where, at the Fermi level, the wave functions are often a combination of *s*- and *d*-like states. The difference simply is in the parameters involved. In *s–d* metals and compounds, the bandwidth, or the "fluctuation frequency," is several volts and considerably larger than the atomic Hund's-rule coupling energies. In the compounds under discussion, the Hund's-rule coupling energy of the *f* states is considerably larger than the fluctuation frequency, so that the local orbitals must first be constructed so as to satisfy atomic spectral rules, and the hybridization must be treated next, perturbatively. An important role is played by the fact that Hund's rule favors integral occupation of a state, as first emphasized by Van Vleck (Van Vleck, 1953). In Table II, we list the characteristic energy parameters in mixed-valence compounds and in *s-d* compounds. What the table shows clearly is that the mixed-valence systems are relatively simple from a theorist's point of view, since the relevant parameters are well separated in energy, while the *s-d* systems, where the parameters are all of comparable magnitude, are a theorist's nightmare. Having said this, we must note that aspects of mixed valence, in the sense used here, are bound to be significant in transition metals, especially when there is a large peak in the density of states near the Fermi level, as for example in Ni.

Another point to re-emphasize, that sets the compounds under discussion apart from others, is the slowness of the ionic fluctuations. All metals have "ionic" fluctuations; in Na, there is on the average one electron per unit cell, but sometimes there is none, and sometimes there are two or three or more. The fluctuation rate increases with bandwidth, however. In the mixed-valence compounds, the fluctuations are slow, so that the local atomic environment is strongly felt in the *f* state.

A few more remarks about "mixed valence" and fluctuating valence: The term "mixed valence" first came into solid state physics, to our knowledge, in reference to compounds like $(La_{1-x}Ca_x)Mn^{3+}_{1-x}Mn^{4+}_xO_3$ investigated by Jonker and van Santen (Jonker and van Santen, 1950). These compounds have the fascinating property that the delocalization of electrons is accompanied by ferromagnetic ordering. Fe_3O_4 at low temperature may also be called mixed-valent because both Fe^{2+} and Fe^{3+} exist physically separated. SmS and other compounds that we will be discussing are different from these in the sense that there is overwhelming evidence that Sm^{2+} and Sm^{3+} do not exist as separate entities either as ordered or as random mixtures. It is possible that compounds like Sm_3S_4 at low temperatures (Bucher *et al.*, 1974; Dernier *et al.*, 1975) are mixed-valent in the same sense as Fe_3O_4. It would be appropriate to expand our terminology and call compounds like Fe_3O_4 and (possibly) Sm_3S_4 "inhomogeneously mixed-valent" and compounds like SmS under high pressure "homogeneously mixed-valent." This article, then, deals with homogeneously mixed-valent compounds, although an interesting question, which we shall come back to in Sec. IV, is the condition under which compounds are homogeneously or inhomogeneously mixed-valent.

We list in Table III some of the materials which have, through one or another experiment, been shown to be mixed-valent in the sense used here. Besides the chalcogenides of Sm, they include compounds of Eu, Tm, and Yb; Ce metal in the α phase; and intermetallic Ce compounds. It is noteworthy that mixed-valence compounds generally form with rare earth elements only at the beginning, the end, and the middle of the rare-earth series. We have already explained why the middle is favored, in terms of Hund's rules. The reason that the beginning and the end of the rare-earth series are also favored is that a closed shell screens the nuclear charge most effectively. Therefore the 4*f* electron in Ce and the 4*f* hole in Yb are relatively loosely bound and not far from the 5*d* configuration.

The qualitative picture presented above, which will be made a little more concrete in Sec. II, is the minimum necessary to characterize the homogeneous mixed-valence phase. Some of the more exotic possibilities for such a phase will be mentioned in Sec. IV. A.

II. MODEL HAMILTONIAN

A. Two-band Hubbard Hamiltonian

Some of the simple ideas about mixed-valence compounds, discussed in Sec. I can be reinforced by a gen-

TABLE II. Characteristic energy parameters for rare-earth mixed-valence compounds compared to transition metal compounds.

	d band in transition metal compounds	*f* band in rare-earth compounds
Bandwidth	~ 5 eV	$<10^{-1}$ eV
Spin–orbit splitting	$\sim 10^{-1}$ eV	$\sim 10^{-1}$ eV
Crystal field splitting	~ 2 eV	$\sim 10^{-3}$ eV
Hund's rule energy	~ 1 eV	~ 1 eV
Electron–electron repulsion (Hubbard's *U*)	~ 5 eV	~ 5 eV

TABLE III. A partial list of known mixed-valence compounds divided into those that are mixed-valent at STP and those that have a transition to the mixed-valent state at high pressures.

STP		High pressure	
	Reference		Reference
$CePd_3$	Gardner *et al.* (1972)	α–Ce	Gschneidner (1961)
$CeSn_3$	Tsuchida and Wallace (1961)	SmS	Jayaraman *et al.* (1975)
$CeAl_3$	Cooper *et al.* (1971)	SmSe	
SmB_6	Nickerson *et al.* (1971)	SmTe	
$EuCu_2Si_2$	Bauminger *et al.* (1973)		
TmSe	Bucher *et al.* (1970)		
$YbAl_2$	Havinga *et al.* (1973)		
Th_xCe_{1-x}	Gschneidner *et al.* (1962)		
$UNi_{5-x}Cu_x$	van Daal *et al.* (1975)		

eralization of the Hubbard Hamiltonian (Hubbard, 1963, 1964) to a two-band situation. The discussion here follows Varma and Yafet (1975) and Sinha and Varma (1975). For a mixed-valence compound in which, say, the f^n and $f^{n-1}d$ configurations are the most probable configurations, we may take the "vacuum" to be given by occupied f^{n-1} states at each rare-earth ion. The f electron Hamiltonian may be taken to correspond to the "zero-bandwidth limit" of Hubbard:

$$H_f = \sum_i H_{fi} ,$$
$$H_{fi} = \sum_{\mu} \epsilon^f C^{+}_{i\mu} C_{i\mu} + \frac{1}{2} \sum_{\mu\nu\sigma\tau} U_{\mu\nu\sigma\tau} C^{+}_{i\mu} C^{+}_{i\nu} C_{i\tau} C_{i\sigma} , \tag{II.1}$$

where i is the site index, $\mu, \ldots, \tau$ are labels distinguishing the various degenerate wave functions of the shell including spin labels, and ϵ^f_{μ} is the energy of adding an extra electron in the multiplet state μ to the f^{n-1} configuration including exchange, spin–orbit interactions, and in principle also the crystal field splittings. In the rare earths the energy difference between different f configurations with the same number of electrons and the same quantum numbers S, L, J is about two orders of magnitude smaller than that for electrons with different number of electrons or different S, L, and J. If we neglect the small multiplet splittings in the zeroth approximation, the f electron Hamiltonian (II.1) corresponds to Hubbard's zero configuration width limit and becomes

$$H^0_{fi} = \epsilon^f n^f_i + \tfrac{1}{2} U (n^f_i - 1) n^f_i , \tag{II.2}$$

where n^f_i, the number of electrons over the f^{n-1} "vacuum" state can be 0, 1, or 2. The distribution of the energy levels of (II.2) will be on a parabola as in Fig. 3. The foregoing discussion of Hubbard, originally made for d electrons, is actually much more appropriate for f electrons.

The important points being made by (II.1) and (II.2) are that the electron–electron repulsion is the largest parameter for an f electron system, followed by Hund's-rule couplings. It is only after these two that f–f transfer or f–d integrals to neighboring atoms must be considered. Strong Hund's-rule couplings tend to maintain integral occupation of atoms, as already emphasized by Van Vleck (1953). This discussion has been used by Hirst (1970) for degenerate magnetic impurities in metals and is being referred to as the Hirst model (Wohleben and Coles, 1973). Coqblin and Blandin (1968) have discussed the same problem earlier.

We may now consider the s-d Hamiltonian. The one-electron Hamiltonian is

$$H_{s-d} = \sum_{\substack{i,j \\ \xi,\xi'}} T^{\xi\xi'}_{ij} C^{+}_{\xi i} C_{\xi' j} , \tag{II.3}$$

where ξ, ξ' denote the "orbital" quantum numbers and spin for the (s–d) electrons. We may, if we like, add to this the correlation energy among d electrons. We shall not pursue that here. The next important thing for our problem is the f–sd transfer Hamiltonian

$$H_t = \sum_{\substack{i,j \\ \mu,\xi}} t^{\mu\xi}_{ij} (C^{+}_{\xi i} C_{\mu j} + \text{c.c.}) . \tag{II.4}$$

Equation (II.4) leads to f-sd hybridization of the f levels with a given electron number. The hybridization leads effectively to an f band. In the mixed-valence compounds, the band structure may look as simple as Fig. 2(a), where we have allowed for some f–f direct overlap, or as in Fig. 2(c), if for symmetry reasons part of the f degenerate multiplets do not hybridize. It must be remembered that the f bands are not one-electron bands in the usual sense, since the maximum occupation on a given atom is limited to 1 if U is very large. The d band may be introduced in Fig. 3 as a relatively wide band compared to the f^n configuration splittings. It may properly be called an f^{n-1} d band. If it overlaps the f^n configuration and the Fermi level overlaps the f^n configurational levels to within the f-sd hybridization energy, we have a mixed-valence situation. The residual interactions between the f and d electrons need to be treated next to obtain a complete description. These can lead to some exotic possibilities, which are mentioned in Sec. IV.A.

It should be noted that even in the semiconducting phase with a gap E_g, there is a small admixture, proportional to t^{fd}/E_g, of the d levels in the ground state.

The above theoretical program is oversimplified and somewhat misleading. The problem is that the hybridization of a Hubbard band (the f band) and a (relatively) free-electron band (the s–d band) cannot be treated by one-electron theory. Since the effective mass of the f

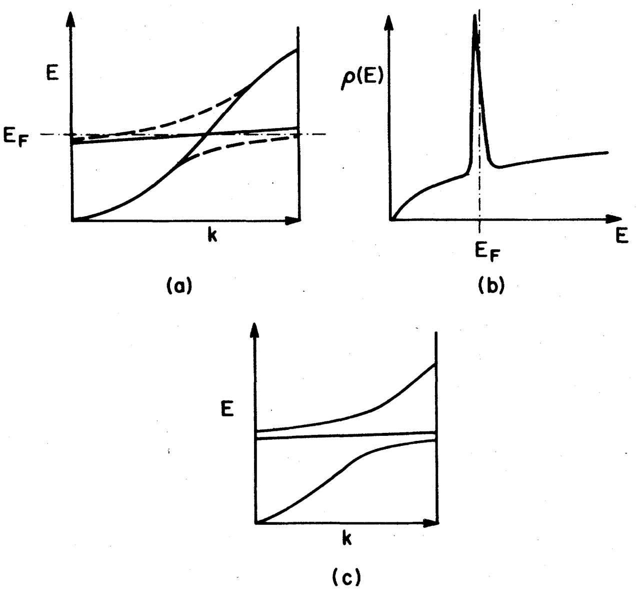

FIG. 2. (a) and (c). Two possible schematic electronic structures for the mixed-valence phase. (b) density of states corresponding to (a).

electrons is much heavier than that of the s-d electrons, we may use a Born–Oppenheimer approximation and conclude that the state of the s-d electrons of energy close to the f electrons depends on the spin configuration of the f electrons. For example, imagine for a moment that the f band is fully spin-polarized in the up-direction. The up-spin free-electron band will then hybridize with the f states and the down-spin will remain totally unaffected. Suffice it to say that the problem of magnetism in the mixed valence compounds and that of the electronic spectrum are inextricably linked together. Hybridization of two bands a and b implies that the "excitonic" correlation function $\langle C^{+}_{\vec{k}\sigma a} C_{\vec{k}\sigma b} \rangle$ has a nonzero value. Thus, formally speaking, one has to evaluate this correlation function for the Hamiltonian $H_f + H_{s-d} + H_t$ to estimate the amount of hybridization and the particle–hole excitation spectrum.

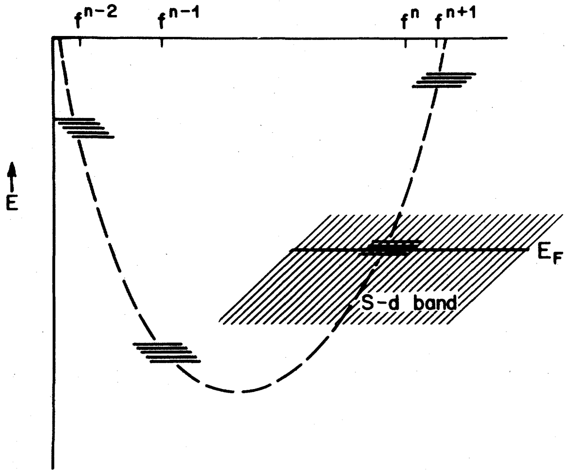

FIG. 3. Hubbard's diagram for electronic energy levels for strongly correlated electronic systems, applied to mixed-valence materials. The multiplet splitting in a given configuration is very small compared to difference in energies of different configurations of f electrons. A wide sd band overlaps one of the configurations.

For a single nondegenerate impurity in a conduction band (the Anderson model), it is possible to write down a good ground-state wave function to represent the hybridization as well as the correlation imposed by $U \to \infty$. It is

$$\Psi = a_0 \Psi_0 + \sum_{\sigma, \vec{k}, < \vec{k}_f} a_{\vec{k}} C^{+}_{f\sigma} C_{\vec{k}\sigma} \Psi_0 ,$$

where Ψ_0 is the Hartree–Fock ground state for the conduction band, and a_0 and $a_{\vec{k}}$ are variational parameters. Such a state satisfies $n_{f\uparrow} n_{f\downarrow} | \Psi \rangle = 0$, and has been shown (Varma and Yafet, 1975) to yield the same behavior for the susceptibility as $T \to 0$, as the correct solution of the Kondo problem (Anderson and Yuval, 1974) for ϵ^f far below the Fermi level and $\epsilon_f + U$ far above the Fermi level. It is, however, hard to construct similar wave functions for the mixed-valence situation where we have an asymmetric Anderson Hamiltonian for each site.

In the mixed-valence phases there may in fact be a small gap of about $(t^2/W - z t_f)$, where W is the s-d bandwidth and t_f the direct f-f overlap, and z the number of nearest neighbors. This is the estimate one arrives at by hybridization in one-electron theory, $-t^2/W$ being the gap for hybridization of the s-d band with a completely flat band. The Fermi level then lies in the middle of a gap, or we may have a semimetallic or metallic situation with the Fermi level lying in the peak of the density of states corresponding to the f "band". In any case the f band carries its multiplet and spin–orbit coupling scheme index, because Hund's-rule and spin–orbit coupling energies are expected to be large compared to t. The crystal field splitting of the f levels may in fact be smaller than t. In this case the crystal field levels will be mixed and cease to be observed experimentally.

An important point to note is that it makes sense to talk of an f band only for $kT \ll t^2/W$. For higher temperatures we have a nondegenerate plasma of f electrons, and the motion of f electrons is diffusive.

Having discussed the formation of a highly correlated "f band" hybridizing with a relatively free s-d band, we must consider the interactions between them.

$$H_{\text{int}} = \sum_{\substack{\xi_1, \ldots \xi_4 \\ i, \ldots l}} V_{\xi_1 i, \xi_2 j, \xi_3 k, \xi_4 l} C^{+}_{\xi_1 i} C^{+}_{\xi_2 j} C_{\xi_3 k} C_{\xi_4 l} ,$$

where $\xi_1, \ldots \xi_4$ denote either f or s-d and the spin indices. We have already included in our discussion the case when all ξ_i refer to the f band. The interactions within the d band are probably not as important as the "excitonic" interactions involving both the f and the s-d bands. These interactions may have relevance to the insulator to mixed-valence metal transition (Falicov and Kimball, 1969). An electron excited from the f band to the d band has a residual interaction with the hole left behind; these excitonic correlations may influence the detailed structure of the mixed-valence state. Some of the possibilities are discussed in Sec. IV. This very important aspect of the problem is yet to be completely sorted out, although some aspects have recently been considered by Khomskii and Kocharjan (1975). The interactions between the f and the d band are crucial in understanding the magnetic behavior in the mixed-valence phase.

B. A simplified Hamiltonian

In order to discuss the hybridization procedure further, we will now consider a model in which the difficulties mentioned above are bypassed. From this tutorial model, one can extract an expression for the average valence and the rms fluctuations about it. In this model the f electrons are considered spinless. Then for the limit $U \rightarrow \infty$, a one-electron Hamiltonian represents the properties of $H^f + H_{s-d} + H_t$ in the "zero configuration width" limit for f electrons (Sinha and Varma, 1975):

$$H^{\text{simple}} = \sum_{i\zeta} E_\zeta C^+_{\zeta i} C_{\zeta i} + \sum_{\substack{i \neq j \\ \zeta, \zeta'}} t^{\zeta\zeta'}_{ij} C^+_{\zeta i} C_{\zeta' j} , \tag{II.5}$$

where $\zeta = f$ or ξ, the set of indices describing the d electrons. The commutation relation

$$[C_{\zeta i}, C^+_{\zeta' j}] = \delta_{\zeta\zeta'} \delta_{ij}, [C_{\zeta i}, C_{\zeta j}] = 0, \text{ etc.} \tag{II.6}$$

automatically excludes more than one f electron per site. We may diagonalize H^{simple} by

$$C_{\vec{k}\lambda} = \frac{1}{\sqrt{N}} \sum_i e^{i\vec{k}\cdot\vec{r}_i} \left[\sum_\zeta A^{\lambda\zeta}_k C_{\zeta i} \right] , \tag{II.7}$$

where λ is a band index, and the quantity $A^{\lambda\zeta}_k$ which expresses the band mixing can be obtained from perturbation theory. Then we have

$$H^{\text{simple}} = \sum_{\vec{k}\lambda} E_{\vec{k}\lambda} C^+_{\vec{k}\lambda} C_{\vec{k}\lambda} . \tag{II.8}$$

The Hartree–Fock ground state for (II.8) is

$$\Psi_{\mathrm{HF}} = \sum_{\lambda, k < k_F} C^+_{\vec{k}\lambda} \left| \cdots (f^{n-1})_i \cdots \right\rangle$$

$$= (N)^{-N/2} \sum_{\substack{i, j, \ldots \\ \zeta_1, \zeta_2, \ldots}} e^{-i\vec{k}_1 \cdot \vec{r}_i} e^{-i\vec{k}_2 \cdot \vec{r}_j} \cdots A^{\lambda_1 \zeta_1}_{\vec{k}} A^{\lambda_2 \zeta_2}_{\vec{k}} \cdots C^+_{\zeta_1 i} C^+_{\zeta_2 j} \cdots \left| \cdots (f^{n-1})_i \cdots \right\rangle . \tag{II.9}$$

Ψ_{HF} represents a linear combination of states representing N atoms in mixtures of f and d configurations.

If we choose the z axis as the axis of spin quantization and we assume that the matrix elements $t^{\zeta\zeta'}_{ij}$ are the same for spin-up d electrons as for spin-down d electrons, we can infer from H_t that, in this model of spinless f electrons, only the x-spin component of the $s-d$ electron band hybridizes with the f electrons. It follows that no gap is introduced in the electronic spectrum.

The expectation value of the f character at the ith site in the Hartree–Fock ground state is homogeneous in the crystal and is given by

$$\langle n_f \rangle = \frac{1}{N} \sum_{k < k_f} A^{\lambda f *}_{\vec{k}} A^{\lambda f}_{\vec{k}} . \tag{II.10}$$

Thus the hybridization parameters determine the averaged "valence" of the rare earth. We may also calculate the fluctuation in the number of f electrons on each site to be

$$[\langle n_f^2 \rangle - \langle n_f \rangle^2] = \langle n_f \rangle (1 - \langle n_f \rangle) . \tag{II.11}$$

As far as the valence state is concerned, Eqs. (II.10) and (II.11) characterize it very well in terms of the stationary (ground) state of the problem. If a nonstationary state is prepared in some experiment, say an integral valence on a given atom rather than a mixed valence, then as in any hybridization problem, the valence will fluctuate at a rate given by the hybridization parameter t^{fd}_k (transform of t^{fd}_{ij}) suitably averaged over the band.

Many experiments have been interpreted to provide a time scale of fluctuations. This should be understood only to provide a measure of an average t_k. The results of any experiment involving transitions between the ground state and excited states, such as those seen by x-ray photoelectron spectroscopy (XPS) and inelastic neutron or light scattering experiments, will depend upon the magnitude of the hybridization energy relative to the energy differences between the various states involved (and the width of the transition). Thus, for instance, in XPS measurements on Sm chalcogenides, the transitions involve large energy differences, corresponding to the difference between the ground state and excited states of the f^6 and f^5d configurations of the Sm ion. Two distinct sets of lines are observed, corresponding to distinct valences, because these states are separated from each other and the ground state by energies far greater than the hybridization energy and the resolution of the experiment. If, on the other hand, an experiment looks at differences less than or about the hybridization energy, no distinct structure associated with the two different valences should be observed. Usually these arguments are given in terms of time scales. The discussion in terms of the energy scales is equally instructive and perhaps amenable to a more precise development.

Static experiments, such as lattice constant and isomer shift measurements, that are determined by the amount of f character, should show a mixed valence given by (II.10) with effectively an extra width (the Debye–Waller factor in the case of the lattice constant) introduced by the f fluctuations given by (II.11).

C. Coupling to the lattice

In the rare-earth chalcogenides, the coupling to the lattice is extremely important, since the ionic radii of different valences often differ by over 10% and the lattice constants are determined by the valence. We can approximately represent the linear part of this coupling by

$$H_{\text{el-lattice}} = \sum_i \tilde{g}\,(1 - n_{fi})(b_i + b_i^\dagger) \ , \qquad \text{(II.12)}$$

where b_i are the annihilation operators for (Einstein) phonons at site i. With $\tilde{g} > 0$, an effective compression of the cell i is obtained if the atom at that site loses its f character. This has an important bearing on the insulator-metal transition in the rare-earth chalcogenides. Couplings of the type (II.12) will renormalize the f-sd transfer integrals of (II.4), and lead to a polaron like depression of the occupied part of the sd band.

D. Coherent configuration fluctuations

We have obtained an approximate ground state, Eq. (II.9), of the mixed-valence systems by projecting out all but the two most probable f configurations by means of Eq. (II.6) and then taking into account the hybridization between the f and the d bands by defining $C_{k\lambda}$ as in Eq. (II.7). The result is to give an average mixed valence in the ground state through Eq. (II.10). It is of interest next to discuss the excitation spectra and to see if there are any features in them which are peculiar to the mixed-valence systems.

The mixed-valence systems will of course have the usual incoherent particle-hole excitation spectrum. The excitation spectrum in metals at long wavelengths is usually predominantly coherent, being of the charge density fluctuation or plasmon character. Because of the long-range nature of the Coulomb interaction, the plasmons have a finite energy at $q=0$. In the mixed-valence systems, we have both the very heavy f and the much lighter s-d electrons near the Fermi surface. It is interesting to speculate that in this situation, besides the coherent in-phase motion of the f and s-d electrons (the usual plasmon), a coherent out-of-phase motion of the f and s-d electrons is possible.

The in-phase oscillations of the f charge density and the s–d charge density are the usual plasmons; the out-of-phase oscillations are the possible new mode. The physics of the new mode is akin to that of longitudinal acoustic (LA) waves in metals. The much lighter electrons screen the ions so that the ion plasmon oscillations are replaced by the LA modes. Similar modes are seen in gaseous plasmas, where they are referred to as ion-acoustic waves. In connection with two species of electrons in solids, the idea of such a mode arose in transition metals and their compounds (Pines, 1956). However, no firm evidence of the existence of such a mode is available in such materials. We believe that the possibility of the existence of such a mode is much higher in the mixed-valence compounds because the ratio of the masses of f electrons to the s–d electrons in these compounds is much larger than the ratio of the masses of the d to the s electrons in transition metals. A theory for the mixed-valence compounds has been worked out (Sinha and Varma, 1975) in a model in which the f electrons are spinless. Here we merely sketch the result in the free-electron approximation. The plasmon frequency is usually given by

$$\omega^2 = V(q)\chi(q) \ , \qquad \text{(II.13)}$$

where $V(q)$ is the potential, and $\chi(q)$ is the polarization. For a Coulomb potential and free-electron polarization, this yields $\omega^2 = (4\pi e^2/q^2)(Nq^2/m) = 4\pi Ne^2/m$. But if the Coulomb interaction between the heavy particles is completely screened by the lighter electrons, $V(q) = 4\pi e^2/(q^2 + k_s^2)$, k_s is the Thomas–Fermi screening length of the lighter electrons, and we get in the long wavelength limit

$$\omega_q^2 = (4\pi e^2/k_s^2)(N_h q^2/m_h) \simeq (v_h v_l) q^2 \ , \qquad \text{(II.14)}$$

where N_h, m_h, and v_h are the density, the mass, and the Fermi velocity of the heavy electrons, respectively, and v_l the Fermi velocity of the light electrons. The Landau damping of this new mode, which may be termed the f-sd acoustic wave, can be shown to be proportional to $(v_h/v_l)^{1/2}$. For temperatures of the order of or greater than the f-electron bandwidth, where the motion of f electrons is diffusive, this mode will be overdamped.

If such a mode exists, it should have important bearing on the nature of the phase transition to the mixed-valence phase, as we will discuss in Sec. IV, and also on the elastic properties of the mixed-valence phase as discussed by Sinha and Varma.

It is also worth noting that the high density of (f) states at the Fermi surface should affect the phonon spectra of the mixed-valence phase significantly. This has, however, not been worked out yet.

III. EXPERIMENTAL RESULTS AND RELATED DISCUSSION

In this section, we will briefly summarize some of the experimental results on mixed-valence compounds and comment on their significance. Where convenient (and possible) we give a discussion of the experimental results right after they are presented. The experiments have been selected on the basis of the light they shed, in our opinion, on the mixed-valence states. A thorough review of the experimental results is certainly not intended here.

A. Lattice constant measurements under pressure

At atmospheric pressure, all the rare-earth chalcogenides form in the NaCl structure and the lattice constant is given quite accurately by the sum of the ionic diameter of the rare-earth ion and the chalcogen ion. Figure 4 gives the lattice constants of the rare earths. The ionic radii of the 2+ state of a rare earth is larger than that of the 3+ state, often differing more than 10%. Sm, Eu, Yb (and TmTe) occur as 2+ (and therefore are insulators); the lattice constants of their chalcogenides are higher than those of other rare earths which occur as 3+ and are metals. These curves have been in fact used to obtain a value for the mixed-valence ratio R from the measurement of the lattice constants, as we will explain below.

The P–V relationship of the Samarium chalcogenides at room temperature is shown in Fig. 5. SmS has a discontinuous drop in the volume at a pressure of about 6.5 kbar accompanied by a change in color from black to golden yellow; SmSe and SmTe have similar changes occurring continuously in the range 10–50 kbars, and

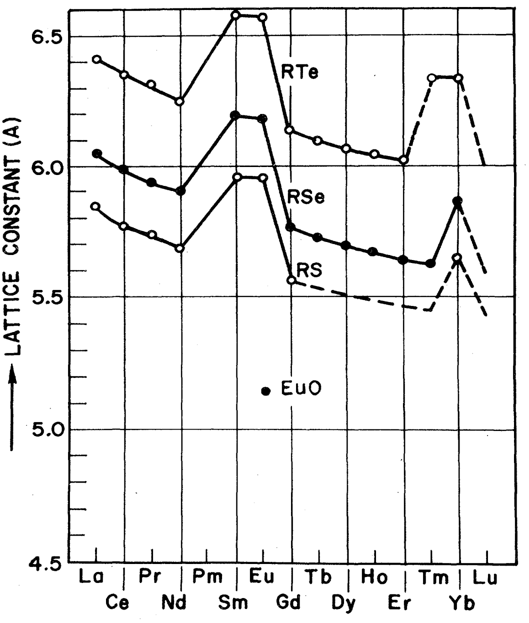

FIG. 4. The lattice constants of rare-earth compounds plotted to illustrate relation of lattice constant to ionic state of the rare earth.

SmS_xSe_{1-x} alloys have transitions which change from discontinuous to continuous as x is reduced (Bucher and Maines, 1972). We have here a metal insulator transition due to the overlap of the d band with the f band under pressure. The f character of the electrons is reduced, but as long as the pressure is not so high that the Fermi level is below the f "band", it is not entirely eliminated. Since valence here is defined in relation to the number of f electrons, a mixed-valence situation results, the valence lying between 2+ and 3+. From Fig. 4 we can, by interpolation, read off what the lattice constant would be for a pure Sm^{3+} chalcogenide metal. By linear extrapolation between the lattice constant of a 2+ and a 3+ chalcogenide, the mixed-valence ratio at the measured volume has been deduced (Jayaraman *et al.*, 1975a).

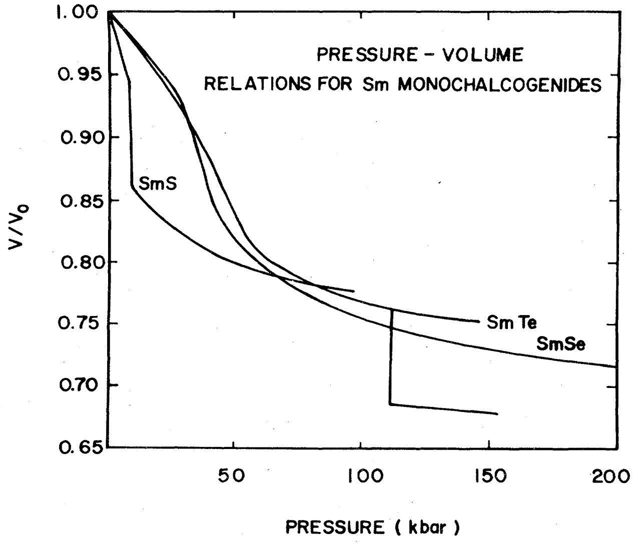

FIG. 5. Measured $p-V$ relation in samarium chalcogenide at room temperature (Jayaraman *et al.*, 1974). The transition in SmTe at about 110 kbar is from the NaCl to CsCl structure and not relevant here.

We now briefly discuss the relationship of lattice constants and valence. If a_2 and a_3 are the lattice constants of the 2+ and 3+ states, respectively, and n_2 and n_3 are the average fraction of 2+ and 3+ character of the atoms, then $R=n_3/n_2$ has been deduced from the measured lattice constant by

$$a=n_2a_2+n_3a_3 \; . \qquad \text{(III.1)}$$

This formula is more suitable for a situation in which the system is a mixture of 2+ (big balls) and 3+ (small balls) ions. Mössbauer experiments which we will soon discuss clearly show that the valence distribution is uniform throughout the sample. In such a situation if $V_2(a)$ is the potential energy distribution of the 2+ rare earth and $V_3(a)$ that of the 3+ rare earth, the lattice constant a is better given by

$$\frac{\partial}{\partial a}\,(n_2V_2(a)+n_3V_3(a))=0 \; . \qquad \text{(III.2)}$$

In general, (III.2) yields a lattice constant larger than (III.1) for the same R. Conversely, for a given measured a, (III.1) gives a lower limit on R. The deductions of valence ratio from measured lattice constants is further complicated by any nonlinear dependence of volume on valence.

In the metallic state, not only is the average f-electron density reduced, there are also larger f-electron density fluctuations due to the increased f-electron bandwidth. Their effect on the lattice constant should be such as to lead to some extra diffuse scattering in the x-ray experiments. The intensity of this scattering should be proportional to Eq. (II.11). Also the mean square displacement of the atoms will be larger in proportion to (II.11).

The $P-V$ diagrams of Fig. 5 raise the important question: why is the insulator-to-metal transition discontinuous for SmS and gradual in SmSe and even more gradual in SmTe? At this point, however, low-temperature experiments have not been performed in SmSe and SmTe so that we do not know whether we are merely above the critical temperature for SmSe and SmTe. This is an important point because if the insulator-to-metal transition is of the Mott type, it must be discontinuous at least at $T=0$. We shall elaborate on this point later and also note that there are ways of getting the insulator-to-metal transition through f-electron–lattice coupling, where even at $T=0$, the transition is continuous for some choice of the parameters (even though no change in symmetry is involved). Another important point which bears closer experimental scrutiny is whether there is any pretransitional softening of the lattice in SmS, i.e., whether $|dV/dP|$ becomes large just before the transition. For a Mott transition this would not, in principle, be the case.

Since we are focusing now on the difference in the P-V diagrams of SmS, SmSe, and SmTe, it is a good place to discuss some "chemical" differences in these compounds. In Table IV we list the ionic radii, lattice

TABLE IV. Some experimentally determined parameters for samarium chalcogenides.

	Lattice constant in the semiconducting phase	Semiconducting gap E_g at zero pressure	$\frac{dE_g}{dP}$ meV/kbar
SmS	5.97 Å	~0.1 eV	−10
SmSe	6.22 Å	0.5 eV	−11
SmTe	6.60 Å	0.7 eV	−11.9
		Ionic radii Å	
	Sm^{2+}	1.14	
	Sm^{3+}	0.96	
	S^{2-}	1.84	
	Se^{2-}	1.98	
	Te^{2-}	2.21	

constants, the insulating gap at atmospheric pressure, and the rate of change of the gap with pressure. The energy of ionic solids in the NaCl structure is least when spheres drawn in this structure, with the ionic radii of the components, touch each other. In the samarium chalcogenides, the arrangement is as shown in Fig. 6; the cations touch the anions but do not touch each other. The anions are thus under an internal pressure. This mismatch is greatest for SmS and least for SmTe. One can therefore expect the largest nonlinear lattice effects with change in valence in SmS. The smaller gap in SmS can be attributed partly to the raising of the f levels due to this internal pressure, and partly, of course, to the larger d band crystal-field splitting and bandwidth, due to the smaller lattice constant.

Another important difference in going from SmS to SmTe is the increasing polarizability of the s-p bands, leading to a larger static dielectric constant.

B. Phase diagram in the P–T and T–x plane and thermal expansion

In Sms the insulator–metal transition has been traced in the T–P plane (Jayarman *et al.*, 1975a), and the results are shown in Fig. 7. The slope of the phase boundary shows that the metal has *lower* entropy than the insulator in the range measured. It would be desirable to extend these results to lower temperatures to see if the slope changes as expected from the study of the doped materials (some conclusions can, however, be drawn from resistivity measurements discussed later). Recent results (Tonkov and Aptekar, 1974) indicate that the phase boundary of Fig. 7 terminates at a critical point at $T \simeq 700$ °C and 7 kbar.

Dopants of smaller ionic radius have been employed (Jayaraman *et al.*, 1973; Holtzberg, 1973; Tao and Holtzberg, 1975; Jayaraman *et al.*, 1975a) to close the insulating gap instead of applying pressure. If the dopant is of a different valence than the rare earth it replaces, it is an extra complication. In this review we shall not discuss the doped materials in any detail. The insulator–metal phase boundary in the T–x plane for $Sm_{1-x}Gd_xS$ is shown in Fig. 8 and that for $Sm_{1-x}Y_xS$ in Fig. 9. In $Sm_{1-x}Gd_xS$, above about 100 °K, the metallic phase M has a somewhat lower entropy than the insulating phase B, but below about 100 °K the metallic phase has a much larger entropy than the insulating phase B′. There is a small but rapid change in volume in going from B to B′, but whether B and B′ are indeed separate phases is not clear at this point. The transition from B′ to M is observed to be explosive. Similar features are observed in $Sm_{1-x}Y_xS$, with the difference that the critical point is reached at about 600 °K, beyond which the transition is continuous (shown by hatched lines in Fig. 9).

The most significant aspect of Figs. 8 and 9 is the existence of a temperature T_0 below which the metal has a higher entropy than the insulator and above which it has almost the same or a bit smaller entropy than the insulator. We shall discuss this feature again in Sec. IV. At this point we merely remark that from lattice contribution alone the entropy of the metal is smaller than the insulator and that Figs. 8 and 9 seem to indicate that the bulk of the electronic contribution to the entropy of the metal must go to zero as the temperature is increased to about T_0.

The thermal expansion coefficients of these compounds are also anomalous. In Fig. 10, we show lattice constant vs temperature for some x in $Sm_{1-x}Gd_xS$ (Jayaraman *et al.*, 1975a). The general behavior seems to be normal thermal expansion in B, a thermal contraction in B', and an anomalously large thermal expansion in M. Similar results are observed with other dopants. In Sec. IV, we will try to relate these features with the re-entrant nature of the phase diagram.

C. Isomer-shift measurements

The 5s electron density at a given nucleus is increased if a 4f electron is removed from that atom. This leads to a shift, the isomer shift, in the Mössbauer spectra. The average position of the Mössbauer line is related to the average number of f electrons at a site. The linewidth, apart from instrumental resolution, is determined by the root-mean-square fluctuations in the number of f electrons at a site and the fluctuation time (or the hybridization energy). If the aver-

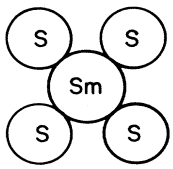

FIG. 6. Manner of touching of the cation–anion spheres in samarium chalcogenides.

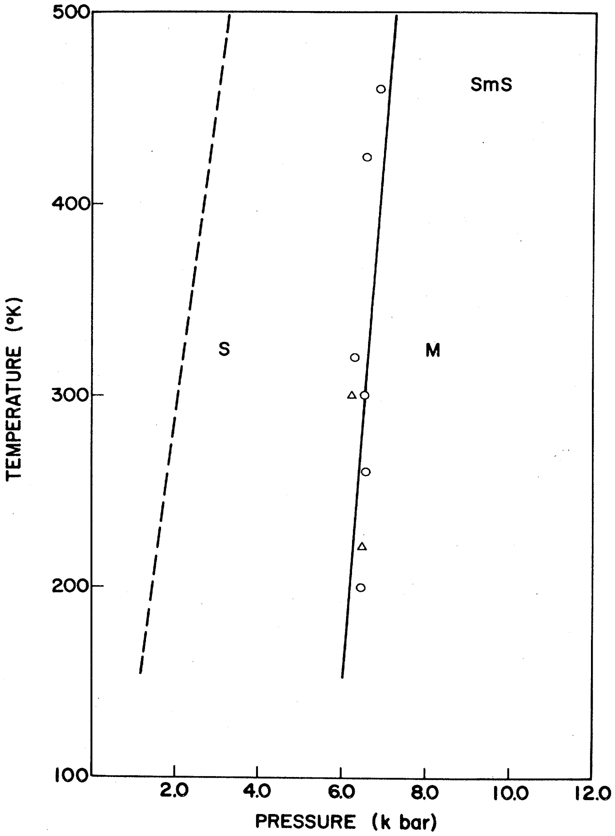

FIG. 7. Phase diagram of SmS in the T–P plane (Jayaraman *et al.*, 1974). The solid line is obtained on increasing the pressure and the dashed line on releasing it.

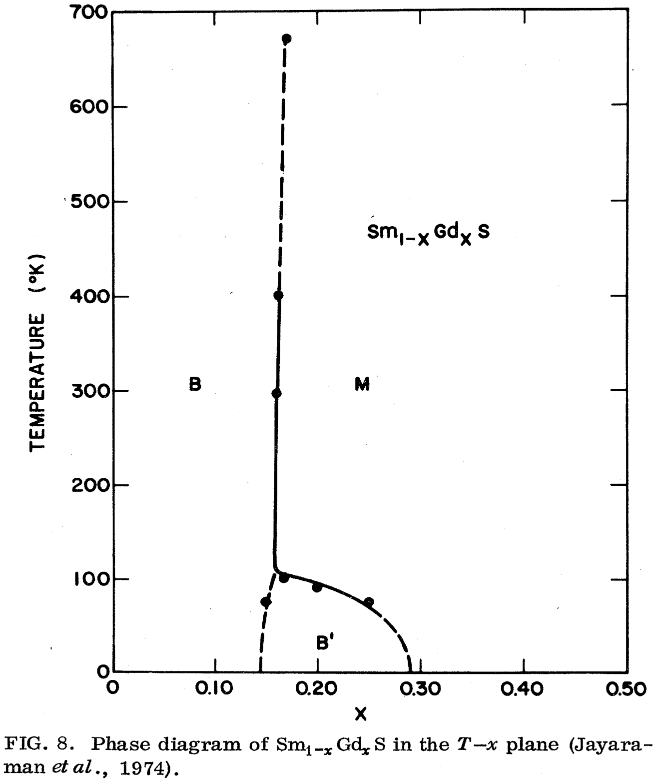

FIG. 8. Phase diagram of $Sm_{1-x}Gd_xS$ in the T–x plane (Jayaraman *et al.*, 1974).

age number of f electrons differs from site to site, two lines would in principle be present, but they may be obscured if the root-mean-square fluctuation is comparable to the difference in the average number, or if the instrumental resolution is inadequate. If one well-defined line is obtained at energies intermediate between the characteristic energies at which the Mössbauer lines of the two valences are expected, one can conclude that the hybridization width of the f band is much greater than the difference in these two energies. In this situation, the Mössbauer line is motionally narrowed. The isomer shift is a very important experiment because, through it, it was conclusively proved that the mixed-valence compounds under discussion are homogeneously mixed-valent.

In these experiments, calibration is done by the positions of the Mössbauer lines in similar materials in which the f electron density is well known from other experiments. The first isomer shift experiment in mixed-valence compounds was done in SmB_6, by Cohen, Eibschutz, and West (1970). A single line is observed with a width such that uniformity of valence can be concluded. Their results are shown in Fig. 11. The isomer shift corresponds to an average configuration of about $f^{5.4}$ or a valence $Sm^{+2.6}$. What is further extraordinary is that, within the resolution of the experiment, the isomer shift is independent of temperature in this compound.

In SmS the experiment has been done at various pressures at room temperature by Coey *et al.* (1974). Again a single line is observed and a configuration of about $f^{5.8}$ or a valence $Sm^{+2.8}$ can be deduced from this experiment. Also, results are obtained for $Sm_{0.77}Y_{0.23}S$ by Coey *et al.* (1974).

One caution in accepting the value given for the mixed-valence ratio by the isomer shift is that the isomer shift is sensitive to any covalent bonding. This is hard to take into account in the analysis of the experiment, but it may be significant. For example, SmS, SmSe, and SmTe, which are believed to have Sm^{2+} at atmospheric pressure, show an isomer shift of -0.73, -0.69, and -0.60 mm/sec, respectively, due presumably to an increasing $5p$ to $6s$ covalent transfer. If we calibrate by

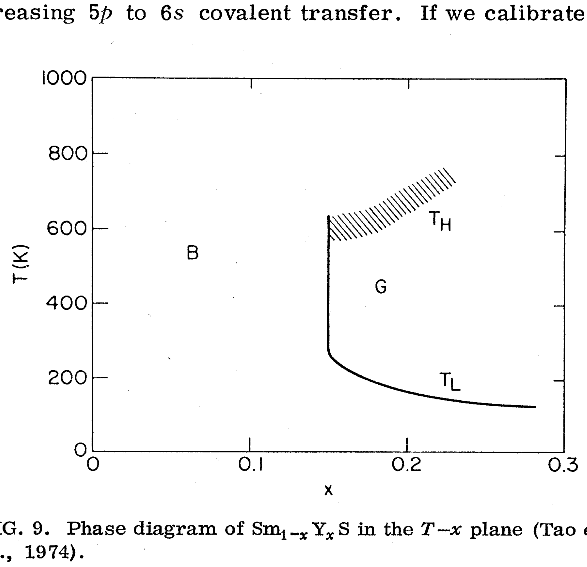

FIG. 9. Phase diagram of $Sm_{1-x}Y_xS$ in the T–x plane (Tao *et al.*, 1974).

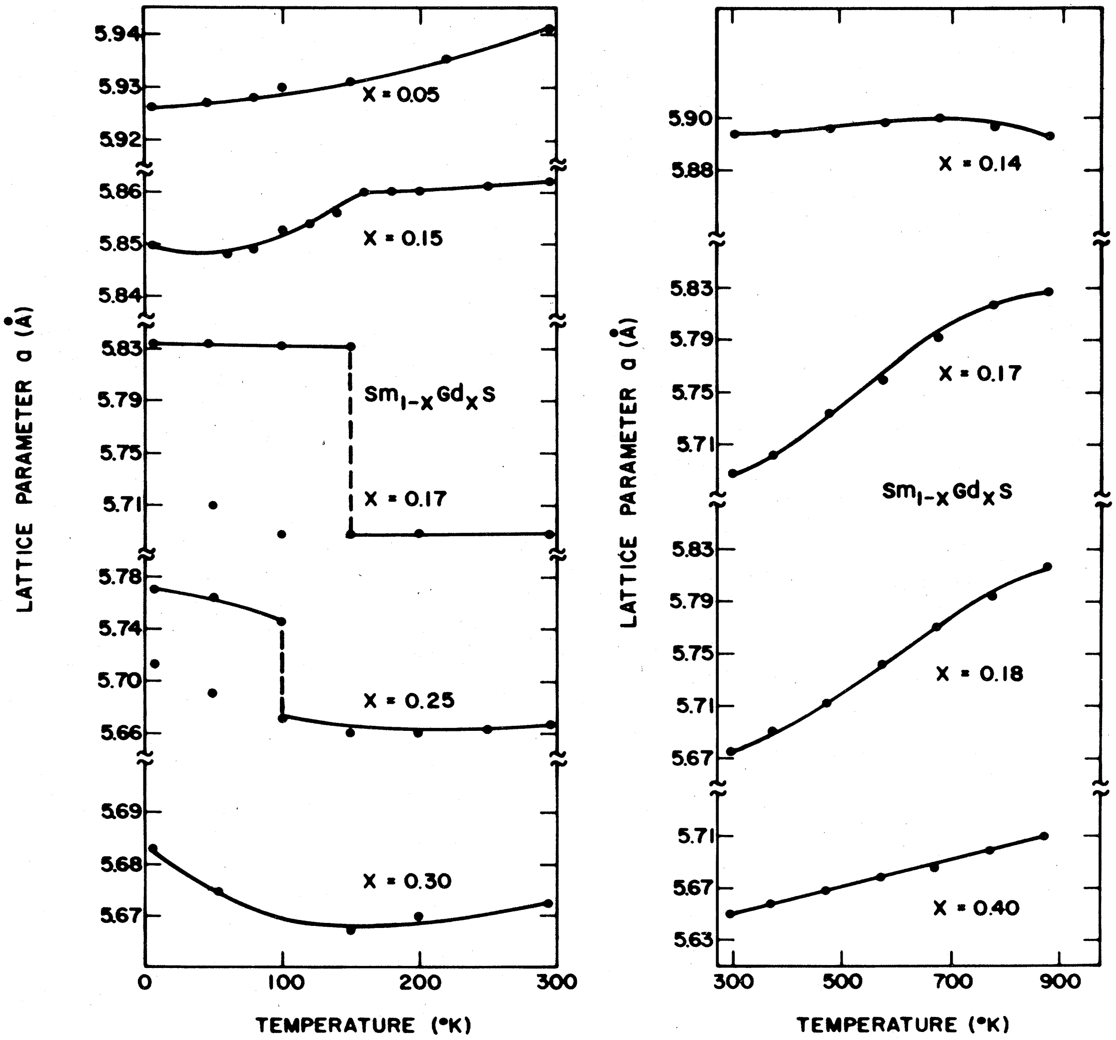

FIG. 10. Lattice constant vs temperature for $Sm_{1-x}Gd_xS$ (Jayaraman *et al.*, 1974).

noting that the isomer shift in the 3+ compound SmF_3 is -0.1, covalency is seen to be a significant effect. We note that some change in covalent character is expected in going to the mixed-valence state.

D. Resistivity

Resistivity measurements in the samarium chalcogenides as a function of pressure exhibit the insulator–metal transition. At room temperature the discontinuous change in resistivity is about a factor of 10. We wish to focus attention on the resistivity in the mixed-valence phase. The resistivity as a function of temperature of SmS (Bader *et al.*, 1973) at two pressures is shown is Fig. 12. The resistivity of SmB_6 (Nickerson *et al.*, 1971), which is mixed-valent at atmospheric pressure, is similar in shape. What is remarkable is that in the "metallic" phase the resistivity rapidly decreases with temperature at low temperatures. This is to be contrasted with the resistivity in $Sm_{1-x}Y_xS$ alloys (Penney and Holtzberg, 1975), shown in Fig. 13. Near the phase transition in the B (black color) phase of Fig. 9, this material is already metallic because Y is trivalent. In going to the G (gold color) phase, the resistivity *increases,* although the number of carriers has increased, and for further increase in temperature it increases as expected of a metal. The increase in resistivity at the transition in this case has been ascribed to the extra electronic scattering due to the f electrons, which are at the Fermi level, in the mixed-valence phase. The upper part of Fig. 9 shows the Hall effect data which support this hypothesis. It would be interesting to see if this behavior of the resistivity persists beyond T_0, when presumably the f-electron contribution to the entropy is depleted. The resistivity of $CeAl_3$ (Andres and Graebner, 1975), which we think is a mixed-valence compound, has been measured down to 15 mdeg. At low temperatures, this has a large T^2 contribution, due, presumably, to scattering of the conduction electrons by the f electrons. This behavior is reminiscent of local spin fluctuation scattering.

The conductivity of SmB_6 and SmS in the mixed-valence phase (Fig. 12) exhibits an activation energy gap at low temperatures which disappears around 100 K, presumably due to the presence of a large number of carriers.

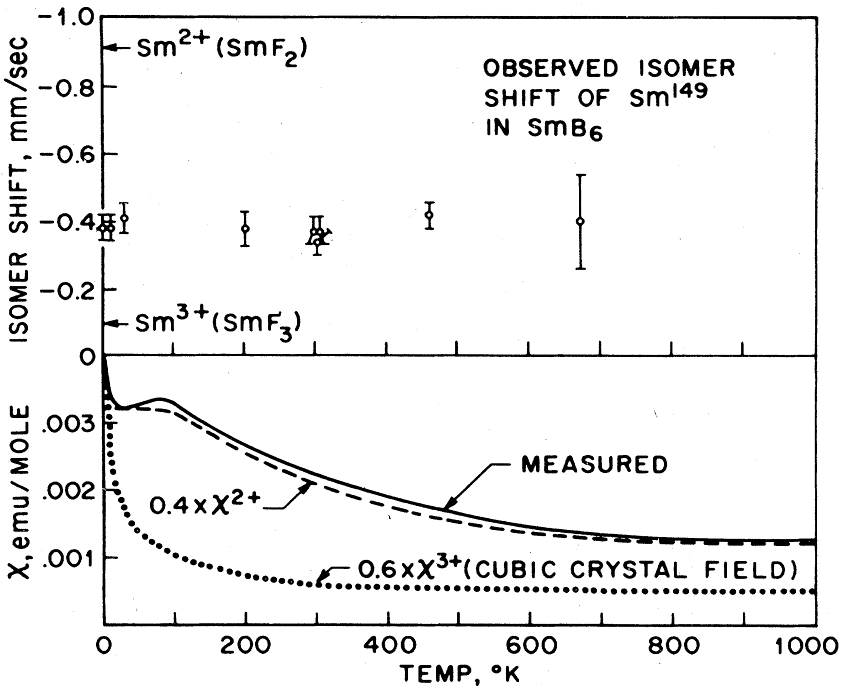

FIG. 11. Susceptibility and isomer shift in SmB_6 (Cohen *et al.*, 1970).

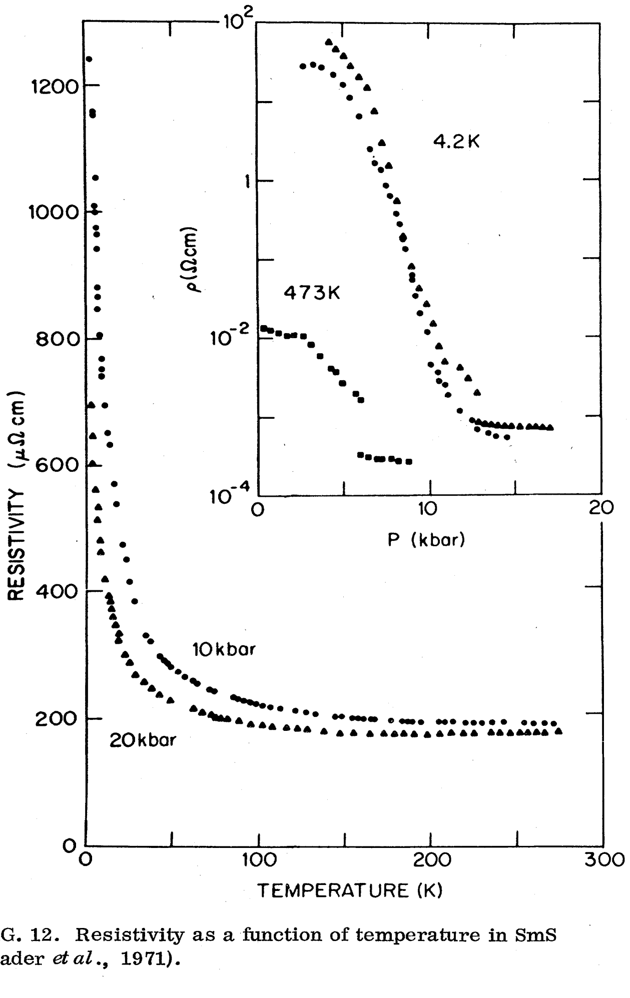

FIG. 12. Resistivity as a function of temperature in SmS (Bader *et al.*, 1971).

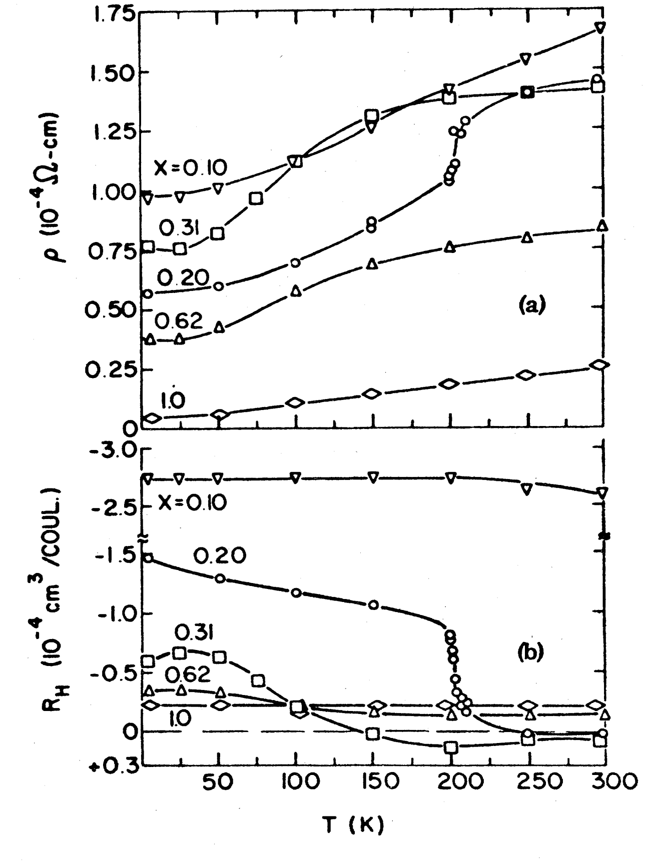

FIG. 13. Resistivity as a function of temperature and the Hall coefficient as a function of temperature in $Sm_{1-x}Y_xS$ (Penny and Holtzberg, 1975).

It is not possible to understand this gap as simply a hybridization gap, since the susceptibility and specific heat data militate against it. One of the possibilities for this gap is discussed in Sec. IV.A. Another idea which needs further investigation is the effect of polaron formation on the resistivity.

Returning to SmS, we may combine the *P-T* information of Fig. 7 and the resistivity at 4.2 K in the inset of Fig. 11 to conclude that pure SmS has also a re-entrant insulator–metal phase diagram.

E. X-ray and ultraviolet photoelectron spectra

Campagna *et al.* (1974a, 1974b) and Pollak *et al.* (1974) have employed the XPS technique, and Freeouf *et al.* (1974) have employed the uv photoemission technique with remarkable results. The XPS technique consists in shining photons of a few keV energy at the solid, and resolving the energy of the outgoing electrons, which to a very good approximation are plane waves. The outgoing electrons have a spectrum which depends on the ionized states left behind in the solid. Consider again SmS. At a few keV energy, the cross section for ionizing d electrons is several orders of magnitude less than that for ionizing the f electrons, so that we may neglect the former process. If an f^6 configuration is ionized, the ground and excited states of the Sm^{3+} configuration, whose energies are known, are seen in the outgoing electron spectrum. If an f^5 configuration is ionized, those corresponding to Pm^{3+} are observed. If both f^6 and f^5 configurations are present in the initial state, two sets of spectra are seen. From the relative intensities of the two sets of spectra the ratio of the f^6 and the f^5 configuration can be deduced. The details are fairly complicated, and we refer to the original articles as well as a brief review (Campagna *et al.*, 1974b) for details.

In the mixed-valence phase, two sets of lines were indeed seen and a mixed-valence ratio which agrees to within 20% with the lattice constant measurements was deduced. It is worth noting that these kinds of spectra can come from both the homogeneous and inhomogeneous mixed-valence states.

Similar results with ultraviolet photon spectroscopy (Freeouf *et al.*, 1974) on the mixed-valence state are also available.

F. Magnetic susceptibility and specific heat

One of the most interesting aspects of mixed-valence compounds is their magnetic susceptibility. Take again, for example, SmS. The ground state of Sm^{2+} has $L=3$, $S=3$, and $J=0$, with the excited $J=1$ multiplet lying about 35 MeV above, in the free ion. Experimentally, the semiconductor exhibits Van Vleck susceptibility, as expected, with the excitation energy closely given by the free-ion multiplet difference. The magnetic excitations have a dispersion (Shapiro *et al.*, 1975; Nathan *et al.*, 1975) which is also easily understood, with an exchange frequency parameter provided by ESR measurements (Birgeneau *et al.*, 1972; Walsh *et al.*, 1974). One would naively expect, from experience with rare-earth metals, that the f^5d configuration would yield a Curie law from the localized f^5 moments (plus a Pauli susceptibility from the d electrons). One would expect the f^5 moments to order eventually at low temperatures due to RKKY interactions. Maple and Wohleben (1971, 1973) have looked at the magnetic susceptibility of SmS in the mixed-valence phase (under pressure). Down to the lowest temperature, no magnetic ordering is found, nor is a Curie-like contribution to the susceptibility present. Their results are shown in Fig. 14. Earlier, similar

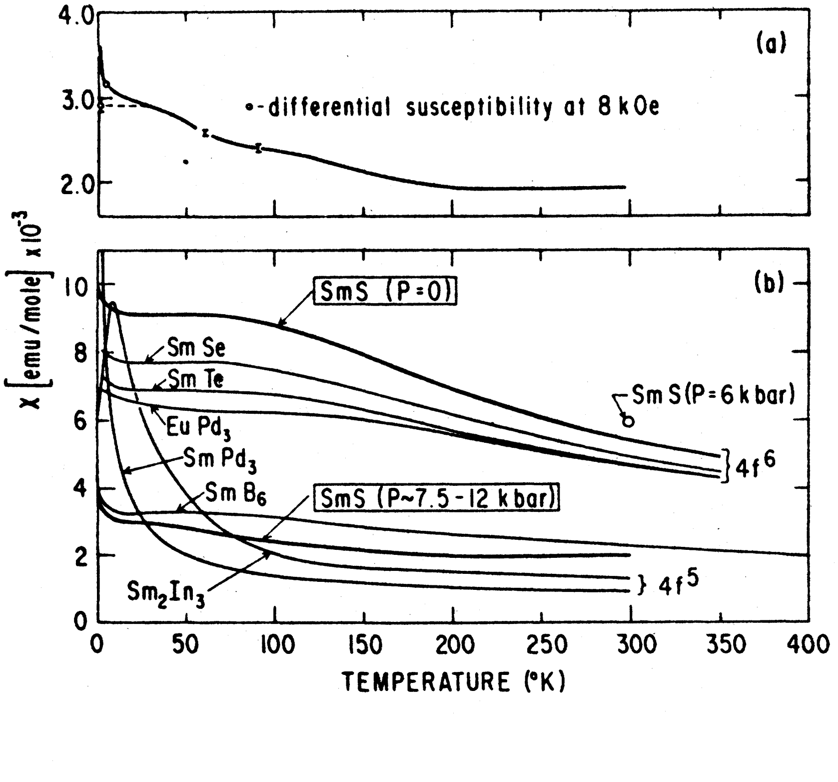

FIG. 14. Temperature dependence of magnetic susceptibility of SmS: (a) in the mixed-valence phase, and (b) at $P=0$ and $P=6$ kbar compared with that of other rare-earth compounds (Maple and Wohleben, 1971).

results were found in SmB_6 (Cohen *et al.*, 1970; Nickerson *et al.*, 1971). Indeed this general behavior is true for all mixed-valence compounds except TmSe, which does have a Curie contribution to the susceptibility, and seems to order antiferromagnetically at about 2 °K. There is one significant difference between TmSe and all the other mixed-valence compounds studied to date. All the others, in the mixed-valence phase, have one or the other valence that is nondegenerate. In TmSe, barring the small crystal field splitting which is relatively unimportant and not even observed (we think, because the hybridization width is larger than it), both the 2+ and 3+ configurations are magnetic configurations.

At this point it is interesting to recall experiments done in La–Ce alloys (Maple, 1973). Pure La is superconducting. Addition of Ce suppresses the transition in a manner suggestive of that done by magnetic impurities. Under application of pressure, as the Ce f level approaches the Fermi surface, superconductivity reappears. This is interpreted as due to the disappearance of the Ce local moment. Indeed the earliest theories of magnetic impurities (Anderson, 1961) gave the result that no local moments are formed when the local impurity levels are very near the Fermi level.

For isolated magnetic impurities it is by now well understood (Anderson, 1973; Wilson, 1975) that for T less than the temperature known as the Kondo temperature T_k, the problem scales to a strong coupling problem, where the local spin is fully compensated by the conduction electrons, and the local moment is quenched. The behavior of the system, conduction electrons plus impurity, at $T \ll T_k$, is simply that of a Fermi liquid (Nozières, 1975). It would seem that in the mixed-valence compounds a similar renormalization is operative to compensate the complete periodic array of all the f levels. This compensation is particularly effective because the f levels lie right at the Fermi level, so that we have a strong coupling situation to begin with.

Motivated by this viewpoint, Yafet and the author (Varma *et al.*, 1975a; Varma and Yafet, 1975b) have calculated the susceptibility for a two-band (f and d) Hubbard model, like the one described in Sec. II, keeping only the f–f interactions at a site. The calculation has been carried in a Green's function decoupling scheme, much like the "prehistoric" calculation by Nagaoka (1965) on the Kondo problem. The results for mixed-valence compounds, in which at least one of the valences is nondegenerate, is that as $T \to 0$

$$\chi(T \to 0) = \mu^2/\Delta, \qquad \text{(III.3)}$$

where Δ is the effective f bandwidth brought about by the hybridization. The first temperature correction is also metal-like, going as $(T/\Delta)^2$. At high temperatures the result is

$$\chi = \mu^2/(T+\Delta), \quad T \gg \Delta. \qquad \text{(III.4)}$$

These calculations qualitatively account for the observed susceptibility in mixed-valence compounds like SmS, $YbAl_3$, $CeAl_3$, etc. They also provide a theoretical basis for the empirical statements of Maple and Wohleben (1971) that the lack of a magnetic moment in the mixed-valence compounds has to do with f–d fluctuations.

Preliminary calculations indicate that this "nonmagnetic" behavior is not found if both the valences in a mixed-valence compound are "magnetic" or degenerate (within an energy Δ). To quench the moment of one valence, the other, degenerate with it, must be "nonmagnetic." This seems to agree with the observations in TmSe.

It is worthwhile at this point to look at the specific heat measurements. The predictions from a theory such as the one by Yafet and the author, for the extra specific heat contribution, are

$$C_V \sim T/\Delta, \quad \text{for } T \ll \Delta. \qquad \text{(III.5)}$$

followed by a maximum around $T \simeq \Delta$ and then a slow dropoff to zero. This may be called the spin-fluctuation contribution to the entropy by the f electrons.

The two specific heat experiments (Nickerson *et al.*, 1971; Bader *et al.*, 1973) have not been carried to high enough temperatures to test the above behavior completely. However, the Δ deduced is consistent with that deduced from the magnetic susceptibility. The data for SmS under pressure are shown in Fig. 15. Some evidence for a maximum in the excess specific heat can be discerned here.

The specific heat results are very relevant to the shape of the metal-insulator line, in the P (or x) $-T$ plane. One may associate the position (T_0) of the change in the sign of the slope of this line, with roughly the temperature at which the previously described excess specific heat goes to zero. (More on this later.) Also, in the mixed-valence phase, one can, in general, expect a different behavior of the resistivity below and above this point. At very low temperatures, the resistivity must vary as T^2, as noted by Mott (1974). This behavior is observed in $CeAl_3$. As already mentioned, SmB_6 remains a bad actor in this respect and its behavior is not at all understood.

Although, with the calculation mentioned, the observed

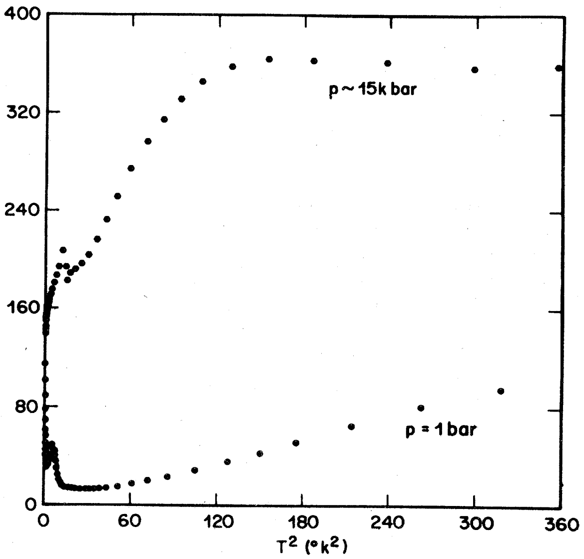

FIG. 15. Specific heat of SmS as a function of temperature at atmospheric pressure and in the mixed-valence phase (Bader *et al.*, 1971).

low-temperature behavior can be qualitatively accounted for, it would be fair to say that the problem itself is not completely understood. After all, although the Nagaoka type solution is good enough to help us understand the low-temperature properties of a magnetic impurity in a metal, considerably more work was required before the renormalization processes operating in the Kondo problem were "understood." The f-band renormalization in the mixed-valence compounds remains to be similarly understood. We believe the answer may well lie in the possibility that with the f levels lying at the Fermi level, the scattering of a conduction electron by a given f level scales to the strong coupling limit much faster than the scaling of the interaction between two f levels through the conduction electrons. This would permit the f spins to remain a "spin-liquid" down to $T \rightarrow 0$.

IV. THEORY OF THE PHASE TRANSITION

A. The homogeneous vs the inhomogeneous mixed valence state

An interesting question is why the average f-electron density in the compounds under discussion is uniform, i.e., why in a compound like SmS a distinct species of 2+ and 3+ ions does not arise in the mixed-valence phase. The latter happens, for example, in Fe_3O_4 at low temperatures. The 2+ and 3+ ions may in principle occur spatially disordered or form some kind of super lattice. Mott has discussed this question briefly. The first point is, of course, that Fe_3O_4 can remain an insulator in the inhomogeneous mixed-valence state, while SmS cannot. Further, in the inhomogeneous mixed-valence state, the conduction electrons will, in general, have a larger kinetic energy. The conduction electrons also screen the f electrons strongly—this is also a factor against the inhomogeneous (disordered or ordered) state. But as important as any of these considerations, in our opinion, is the fact that in the rare-earth chalcogenide the local volume is tied to the local ionic radius. An inhomogeneously mixed valent state would lead to structures which would cost a lot of energy because of departures from the NaCl structure. In other words, the bonding requirements of the core electrons preclude formation of structures favorable to inhomogeneous mixed-valence phases.

The ordered, inhomogeneous, mixed-valence phase—localized f^6 configurations ordered in space in a sea of d (plus f^5) electrons—has the physics of a Wigner lattice. Experimentally, there is firm evidence against its occurrence, and we have rationalized this by the above arguments. It is worth pointing out, however, that the large difference in the ratio of the f and the s–d masses would, by itself, favor such a state strongly. The reason is that r_s is given by

$$r_s = (3/4\pi\rho)^{1/3} a_0^{-1}, \qquad \text{(IV.1)}$$

where ρ is the density and $a_0 = \hbar^2/me^2$. Therefore, we have a large r_s for the f electrons (holes) and a small enough r_s, comparatively, for the d electrons so that the latter could be regarded as a uniform background. Potential energy dominates for particles of large r_s in a uniform background, and Wigner lattice formation is possible.

Experiments also seem to rule out another exotic possibility—an ordered array of excitons (f^5 and d bound together) in a sea of f^6 configurations. (This presumably would be called the Excitonic Insulator state.) The arguments given in the first paragraph of this section may also be used to rationalize its nonoccurrence.

A possibility that the experiments do not seem to rule out is a liquid, rather than a crystal, of these excitons. A liquid state is again favored because of the large difference in the mass of the constituents of the excitons, since that promotes multiexciton binding. Such a state is more likely to be of indirect excitions, because f^6 has $J = 0$, and therefore f^6 to f^5d transition on the same atom is not possible. Such a state would have characteristics not in disaccord with the lattice constant. Mössbauer, and XPS–UPS data. The susceptibility and specific heat in such a model need to be worked out. These excitons must not be interpreted literally. They are in the nature of strong excitonic correlations, which are already present in the theory for the susceptibility (Varma and Yafet, 1976). The attractiveness of such a model as a refinement of the simpler—Occam's razor—model, which we have discussed in Sec. II, is that there would be a gap for the conductivity, which would be screened out by the free carriers at higher temperatures, and therefore the observed resistivity in SmS under pressure, and in SmB_6, could be understood. Presumably the presence of a large number of other free carriers, as in $CeAl_3$ or trivalently doped Sm chalcogenide, would also screen the excitons, so that the simpler picture is recovered. Again this would be in accord with the resistivity in such substances.

B. Insulator-to-metal transitions

To develop a mean field theory of the metal–insulator transition at $T = 0$ in the rare-earth chalcogenides, we must write down an expression for the energy as a function both of the average number of conduction (s–d) electrons per atom, Z, and the average volume per atom, V. The contribution to the energy can be written as a sum of contributions which are primarily electronic in nature and those that are primarily of lattice origin:

$$E(V, Z) = E_e(V, Z) + E_l(V, Z). \qquad \text{(IV.2)}$$

Since the volume depends strongly on the valence of the rare-earth ion, this distinction is hardly precise. The contribution to metal–insulator transitions in general, due to electronic correlations, has been extensively discussed in the literature. We shall, of course, touch on that. Here, we first wish to emphasize the special features of the transition in the rare-earth chalcogenides which may be said to arise from lattice-like effects. As already mentioned there is a large (over 10%) difference in the lattice constant for a solid composed of $f^{n-1}d$ ions and a solid composed of $f^n d$ ions. This difference contributes very significantly to the difference in energy between the two configurations because the materials we are discussing are very hard, with a bulk of modulus of about 500 kbar. Thus the conversion to an f^{n-1} atomic configuration, by promotion of an f electron to a d state, leads to a collapse of the lattice around the f^{n-1} configuration, leading then to a $P\Delta V$ reduction in the energy of $f^{n-1}d$ state relative to f^n. This tends to further increase the density of such excitations, and so on. The process is limited by the fact that the density of states of d electrons is small compared to that of the f states, so that increasingly larger energy is required to create new $f^{n-1}d$ states. A microscopic derivation of this picture has been given by Heine and the author (Varma and Heine, 1975). Related work on this problem has been done by Hirst (1974).

Let us consider the lattice-like contribution to the energy first. We can write

$$E_l = B(V)(V - V_0)^2/2V_0, \tag{IV.3}$$

where we have included the empirically observed variation of the bulk modulus on the volume (Jayaraman *et al.*, 1974)

$$B(V') = B(V)(V/V')^{\gamma} \tag{IV.4}$$

with $\gamma \simeq 1.3$. We define V_0 such that it would be the average equilibrium volume per rare-earth atom if E_l were the only contribution to the energy. V_0 thus depends on the average valence Z, and we write this dependence as

$$V_0 = V_2(1 - Z) + V_3 Z + V_4 Z(1 - Z). \tag{IV.5}$$

In (IV.10), V_2 and V_3 are the volumes for the solid composed of 2+ and 3+ ions, respectively (with samarium chalcogenides in mind), and we have introduced a nonlinearity parameter V_4. The physics of the nonlinear term is that there will be an elastic interaction energy between ions of the same size. This interaction energy is always attractive if the lattice is purely harmonic, leading to a contraction of the lattice. The anharmonic terms can make a repulsive contribution to the interaction energy (Anderson and Chui, 1974).

The one-electron contributions to $E_l(V, Z)$ are the promotion energy $E_g(V)$ from the f levels to the conduction band and the banding energy E_B. To this we must add the nonlinear terms arising from exchange and correlations, E_{xc}:

$$E_l(V, Z) = Z[E_g(V)\,\theta(E_g) + E_B] + E_{xc}, \tag{IV.6}$$

where $\theta(E_g) = 1$ for $E_g(V) > 0$, (i.e., bottom of conduction band above the f level), and $\theta(E_g) = 0$, for $E_g(V) < 0$. Thus in (IV.6), the effects arising from hybridization are being ignored. Experimentally the coefficient of the linear term in the variation of E_g with volume is known through spectroscopic data. Its nonlinear dependence may be taken to be of the same form as the bandwidth of the d electrons. The total electronic energy must, of course, be calculated with the requirement that the chemical potential of the f electrons coincides with the chemical potential for the conduction electrons.

Given the total energy as a function of the average fractional valence Z and the volume V, we can calculate the P–V relationship by requiring that at equilibrium

$$\partial E(Z, V)/\partial V = 0, \quad \text{for } Z > 0. \tag{IV.7}$$

This provides us with a relationship $Z(V)$ at equilibrium. For the equilibrium position to be stable, the determinant of the second derivatives of E with respect to Z and V must be positive. This condition can be easily shown to be equivalent to the condition that $dP/dV < 0$. We therefore require

$$-\frac{dP}{dV} = \frac{\partial^2 E}{\partial V^2} - \frac{(\partial^2 E/\partial Z \partial V)^2}{\partial^2 E/\partial Z^2} > 0, \tag{IV.8}$$

for stability. Inserting $Z(V)$ obtained from (IV.7) into (IV.8) and integrating, the equation of state P vs V can be calculated.

These calculations were done numerically using the parameters given in Table V. The contribution E_{xc} was ignored. The d bandwidth at atmospheric pressure was taken to be 2.5 eV, consistent with the band structure calculation by Davis (1971). Apart from this we really have only one undetermined parameter, V_4, for each material. The calculated $P - V$ curves given in Varma and Heine (1975) agree with experiment to about 10%. This agreement is not as spectacular as one might think. After all, the initial slope and the slope after the transition region are more or less fixed by the empirical relation given by Eq. (IV.3). We are merely fitting the transition region, which can easily be fitted by a two-parameter curve. We choose one of them for each material, and seem to get the other one correctly from the theory.

We do not require a repulsive nonlinear contribution (Anderson and Chui, 1974) for the transition. The trend in V_4 in going from SmS to SmTe is what one would expect from elastic interactions using the arguments about ionic mismatch given in Sec. III.A. It is hard to estimate the magnitude of V_4 from microscopic theory. In principle, V_4 also parametrizes the effects of short-range electronic correlations, as we discuss below.

In these calculations, we find a finite value of Z before the transition even in SmS. This is due to the $Z^{5/3}$ contribution of the banding energy. Associated with this is a small pretransitional softening of the lattice. These calculations are actually more suitable in the high temperature regime where the difference in the entropy of the insulator and the metal is negligible.

A theory of the above kind, in which part of the change of pressure with volume comes about due to the change in Z with volume, also predicts that the Bulk modulus in the mixed-valence phase will be relatively small. The longitudinal acoustic sound velocity in the mixed-valence phase will be therefore relatively low. This has recently been observed (Melcher *et al.*, 1975). We do not expect such an effect on the transverse branch since Z is unlikely to depend much on shear strains.

It is worth pointing out that another phase transition, metal to a better metal, is to be expected at higher pressures in these materials near the point when the bottom of the $s - d$ band is far enough below the f band so that it can accommodate one electron per atom.

TABLE V. Parameters used to calculate the P–V diagram in samarium chalcogenides by Varma and Heine (1975).

	B (kbar)	$\frac{V_2 - V_3}{V_2}$	V_4/V_2	$W(P=0)$ (eV)	γ
SmS	476	0.17	−1.1	2.5	1.3
SmSe	520	0.17	−0.6	2.5	1.3
SmTe	400	0.16	−0.5	2.5	1.3

This is, of course, conditional on a crystallographic transition not occuring earlier.

C. Correlation and exchange contribution to the energy

When an f^6 configuration goes to a f^5 + conduction electron state, the "conduction" electron has of course a residual interaction energy with the hole left behind—the exchange energy. This energy must be calculated in the screening field of the other electrons. This is the basis of Mott's famous theory of metal–insulator transitions. We shall discuss this shortly. Let us first consider the correlation energy. If a small number of f^5d configurations are considered, we should develop a low density expansion for the correlation energy. The leading term in the correlation energy goes as Z^2, representing physically the short-range interaction between the "excitons." This interaction is usually attractive (Falicov and Kimball, 1969). Ramirez, Falicov, and Kimball (1970, 1971) have used this contribution to the energy alone as the driving force for the transition to the mixed-valence phase. It would be hard to understand the enormous volume change at the transition on the basis of such a model. Since V_4 in (IV.4) is an adjustable parameter, and V_2 and V_3 are empirical, we may if we like, simply consider that (IV.3) already includes the contributions of the short-range correlation and avoid introducing an additional parameter.

In the calculation described in (IV.B), the effects due to the lattice were dominant. In Sec. IV.C we will find that the effects of raising the temperature could also be understood as being due to the volume difference of $f^{n-1}d$ and f^n configurations. We are forced to ask why the effects of exchange energy, which are the driving force of the Mott transition, may not be playing a crucial role in the mixed-valence compounds. Consider the Coulomb interaction energy between an electron and a hole in the presence of the conduction electrons. The energy is

$$E_{\text{ex}} = -\int \frac{e^2}{\epsilon(r) r^2}\, dr, \tag{IV.9}$$

where $\epsilon(r)$ arises due to the screening. If we assume the screened potential is Thomas–Fermi like (with k^{-1} the screening radius), then

$$E_{\text{ex}} = -\int dr\, \frac{e^2}{r^2} e^{-kr} \sim -k \sim -Z^{1/6}. \tag{IV.10}$$

Thus the total exchange energy for Z electrons is attractive and varies as $-Z^{7/6}$. Now if we include such a term in our expression for the total energy, it completely dominates the considerations for small Z, since it is the most nonanalytic at $Z=0$. Since it is attractive, it will always lead to a first-order transition.

An exciting possibility, which would spoil the above Mott catastrophe, comes about if the coherent configuration fluctuations (f–sd acoustic waves) discussed in Sec. II are anywhere close to reality. The point is that the d electrons are screened strongly by such fluctuations, in a manner analogous to that for phonons; the effective interaction between a d electron and an f hole becomes retarded, and even changes sign, so that the above Mott argument does not work. The details of this possibility are worked out by Sinha and Varma (1975).

D. Phase diagrams in the T-P or T-x plane

The theoretical effort to trace the metal–insulator transition in the temperature–pressure plane or the temperature–dopant concentration plane has been very slight. Here we shall schematically trace the considerations that lead to instability of the metal or the insulator phase in the T–P and the T–x plane. Extensive experimental results are available for the T–x plane. What is interesting is that the phase boundary in the T–x plane (and probably in the T–P plane) is actually double valued (Figs. 8 and 9). There are also quite anomalous effects in the thermal expansion coefficients quite far away from the transition (Fig. 10).

Let us start by writing down an expression for the thermal expansion coefficient. The dependence of volume on temperature is a result of the direct dependence due to the anharmonicity and also a result of the variation of Z with temperature. Therefore,

$$\kappa = \frac{1}{V}\frac{dV}{dT} = \frac{1}{V}\frac{\partial V}{\partial T} + \frac{1}{V}\frac{\partial V}{\partial Z}\frac{\partial Z}{\partial T}. \tag{IV.11}$$

However, Z, in turn, depends on the volume, since the volume determines the gap E_g in the insulating phase and the Fermi energy E_F (which is pinned to the f level) in the metallic phase. Thus we may write

$$\frac{\partial Z}{\partial T} = g(T)\frac{dV}{dT}. \tag{IV.12}$$

Combining (IV.16) and (IV.17),

$$\kappa = \kappa_0/[1 - g(T)\partial V/\partial Z], \tag{IV.13}$$

where κ_0 is the lattice thermal expansion coefficient when change of Z with temperature is negligible.

We will now sketch how $g(T)$ may be determined. Suppose we are in the insulating phase with a gap $E_g(V,T)$. Then

$$Z(T) = \int_{E_g(V,T)}^{W} d\epsilon\, \rho(\epsilon) f(\epsilon, T), \tag{IV.14}$$

where $\rho(\epsilon)$ is the density of states in the conduction band, $f(\epsilon,T)$ is the Fermi function, and W is the bandwidth of the conduction band. For temperatures that we are concerned with we may take W to be ∞. Ignoring for the moment the higher-lying f levels, we get

$$Z(T) \simeq e^{-E_g/T} y(E_g/T), \tag{IV.15}$$

where $y(x)$ depends upon the band structure and is slowly varying on the scale of the exponential. Then taking into account the fact the E_g also depends on temperature, and using

$$\frac{dE_g}{dT} = \frac{\partial E_g}{dV}\frac{dV}{dT}, \tag{IV.16}$$

we get from (IV.15) and (IV.11)

$$\kappa(T) \simeq \frac{\kappa_0}{1 - \alpha\beta y(E_g/T) e^{-E_g(T)/T}}, \tag{IV.17}$$

where

$$\alpha = -\frac{1}{V}\frac{dV}{dZ} > 0 \tag{IV.18}$$

and

$$\beta = V\frac{dE_g}{dV} > 0. \tag{IV.19}$$

Equation (IV.22) must be solved together with

$$E_g(T) = E_g(0) + \beta\int_0^T \kappa(T')dT'. \tag{IV.20}$$

Generally as E_g/T increases, $y(E_g/T)$ increases. At $E_g = 0^-$, we have an instability for $T = 0^+$ because $\kappa(T)$ is negative, which makes $E_g(T)$ less than zero. As we increase E_g slightly, if the denominator is negative, we will have thermal contraction, which tends to decrease E_g still further, leading to further contraction. The factors $f(E_g/T)$ etc., tend to slow down the contraction (costs more and more energy to populate the d states). By a balance of these factors we can have the denominator going to zero, infinite contraction, and a transition to the metallic state. If E_g is large enough, we will start at low temperatures with a thermal expansion which then removes any instability. The phase diagram from the insulating side at low temperatures is thus as shown by the curve with a negative slope in Fig. 16, $E_g^{\max}$ is a point beyond which only thermal expansion can take place, and there is no transition. If we included the higher-lying f states, the qualitative picture would remain the same, but the instability would occur generally at higher temperatures. By inserting numbers in (IV.17), the above scenario can be seen to be reasonable.

The general feature from the insulating side at low temperatures is: if there is contraction, there will be a metallic transition as T is increased, and the larger the $E_g(0)$, the larger the T_{trans}. If there is thermal expansion then the insulating phase is stable.

We can also trace the line of instability from the metallic side. If there is a thermal expansion, the bottom of the d level moves up relative to the f level, thereby increasing the fraction of occupied f levels. This further increases the volume and so on, till at high enough temperature, $E_g(T) \to 0$, and we have regained a semiconductor. We can write

$$N_d = \int_{-E_c(T)}^{0} \rho(\epsilon)f(\epsilon, T)d\epsilon, \tag{IV.21}$$

where $-E_c$ is the bottom of the condution band relative to the f level (and Fermi level) at 0, and calculate $g(T)$ and $\kappa(T)$ together with

$$E_c(T) = E_c(0) + \frac{dE_c}{dV}\int_0^T \kappa(T')dT', \tag{IV.22}$$

just as we did from the insulating side. The line of instability will look like the line with a positive slope (almost vertical) in Fig. 16, indicating that the smaller the E_g one starts out with, the smaller the temperature required to go to the insulating state.

Here we have merely sketched the line of instabilities to indicate the kind of considerations that go into the transitions. Similar physical arguments have been given by Tao and Holtzberg (1975). The actual phase diagram must be determined from the minimization of free energies, which will presumably eliminate the crossing over of the instability lines discussed above. The nonlinearities discussed in the preceeding section will, of course, play an important role in determing the order of the transition and the details of the phase boundaries. The qualitative features of the argument above seem to be borne out by the experiments, including the predictions of anomalous contractions at low temperatures, and anomalous expansions at high T. At high temperatures, the lattice entropy in the insulating phase must be important enough so that dP/dT is positive, whereas it is less important at low temperatures.

The point in Figs. 8 and 9 where the slope changes sign must be associated with the temperature at which the electronic contribution to the entropy ceases to be important. Specific heat experiments at higher temperatures are needed to verify this assertion.

V. CONCLUDING REMARKS

In this review, the following ideas concerning the mixed-valence phase have been emphasized, which we believe are crucial to further developments in theory:

(1) pinning of the Fermi level by the f levels, the hybridization of the f and s–d states, and the exclusion of states of more than one f electron per atom;

(2) large differences between the f electron and the s–d-electron masses, and the obeying of atomic spectral rules by the f electrons;

(3) strong lattice effects arising from the fact that the NaCl structure prefers lattice constants which are the sum of the ionic radii of the constituents.

The pinning of the Fermi level leads directly to the strong coupling for the interactions of the f and s–d electrons, and consequently strong excitonic correlations. These sd–f correlations have been considered in the theory for the magnetic susceptibility, but the ade-

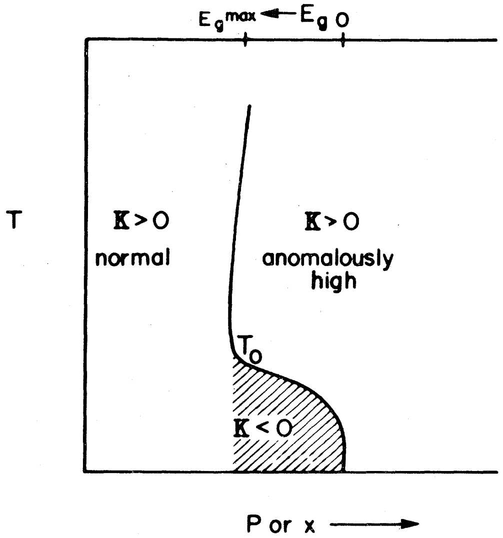

FIG. 16. Schematic phase diagram of $\text{Sm}_{1-x}\text{Ln}_x\text{S}$ showing behavior of thermal expansion coefficient in various regions and showing the point T_0 near where the electronic contribution to the entropy of the mixed-valence phase seems to go to zero.

quacy of the theory for finite temperatures is open to question. Related to this is the question of the specific heat. The turnover of the spin fluctuation contribution to the entropy at $T \simeq T_0$ seems to be required by the double-valuedness of the phase diagram. A proper theory of this turnover is yet to be constructed.

Theory is quite silent on the issue of the resistivity data, of which more at low temperatures would be most welcome. It is possible that the anomalous low-temperature resistivity is related to excitonic *sd–f* correlations. Other experiments that are sorely needed are specific heat measurements at low and intermediate temperatures, and inelastic scattering experiments with energies in the infrared. An infrared reflectivity experiment in TmSe (Ward *et al.*, 1975) has yielded quite mysterious results.[1] The study of phonon spectra in the mixed-valence state should also be quite interesting.

Experiments to determine the phase diagram of SmSe and SmTe at low temperatures are yet to be undertaken, to decide whether the continuous nature of the transitions persists, or whether there is a critical point. Diffuse x-ray scattering and Debye–Walter factor measurements, to see the effect on the lattice displacements of local *f*-electron density variation, would also be quite illuminating.

Experiments to investigate the critical behavior at the transition to the mixed-valence state are beginning to be undertaken (Lawrence *et al.*, 1975). The intermetallic compounds $\mathrm{Th}_x\mathrm{Ce}_{1-x}$ or $\mathrm{La}_x\mathrm{Ce}_{1-x}$, in which these investigations have been undertaken, are very interesting experimentally because the transition is in a very accessible range of temperatures and the shape of the phase diagram (quite different from the samarium chalcogenides) is such as to make the study of the critical region relatively easier.

ACKNOWLEDGMENTS

A number of my colleagues have contributed to my understanding of and familiarity with the mixed-valence compounds. Special thanks are due to P. W. Anderson, R. J. Birgeneau, M. Campagna, R. L. Cohen, V. Heine, A. Jayaraman, D. B. McWhan, S. K. Sinha, and Y. Yafet.

REFERENCES

Anderson, P. W., 1961, Phys. Rev. **124**, 41.
Anderson, P. W., 1973, Comm. Solid State Phys. **5**, 73.
Anderson, P. W., and S. T. Chui, 1974, Phys. Rev. B **9**, 3229.
Anderson, P. W., and G. Yuval, 1973, in *Magnetism*, edited by H. Suhl (Academic, New York), Vol. V, p. 217.
Andres, K., and J. E. Graebner, 1975, Bull. Am. Phys. Soc. **20**, 374.
Andres, K., J. E. Graebner, and H. R. Ott, 1975, Phys. Rev. Lett. **35**, 1779.
Bader, S. D., N. E. Phillips, and D. B. McWhan, 1973, Phys. Rev. B **7**, 4686.
Bauminger, E. R., D. Froindlich, I. Nowik, S. Ofer, I. Felner, and I. Mayer, 1973, Phys. Rev. Lett. **30**, 1053.
Birgeneau, R. J., E. Bucher, L. W. Rupp, Jr., and W. M. Walsh, Jr., 1972, Phys. Rev. **85**, 4312.
Bucher, E., A. C. Gossard, J. P. Maita, and A. S. Cooper, 1969, in *Proceedings of the 8th Conference on Rare Earth Research* (U.S. Govt. Printing Office, Washington, D.C.), 1, 74.
Bucher, E., and R. G. Maines, 1972, Solid State Commun. **11**, 1441.
Bucher, E., K. Andres, F. J. DiSalvo, J. P. Maita, A. C. Gossard, A. S. Cooper, and G. W. Hull, Jr., 1974, Phys. Rev. **10**, 2945.
Campagna, M., G. K. Wertheim, and E. Bucher, 1974a, in *Proceedings of the 20th Annual Conference on Magnetism and Magnetic Materials*, San Francisco, 1974 (AIP Conf. Proc. No. 24), p. 22.
Campagna, M., E. Bucher, G. K. Wertheim, and L. D. Longinotti, 1974b, Phys. Rev. Lett. **33**, 165.
Chatterjee, A., A. K. Singh, and A. Jayaraman, 1972, Phys. Rev. B **6**, 2285.
Coey, J. M. D., S. K. Ghatak, and F. Holtzberg, 1974, in *Proceedings of the 20th Annual Conference on Magnetism and Magnetic Materials*, San Francisco, 1974 (AIP Conf. Proc. No. 24), p. 38.
Cohen, R. L., M. Eibschutz, and K. West, 1970, Phys. Rev. Lett. **24**, 383.
Cooper, J. R., C. Rizzuto, and G. Olcese, 1971, J. Phys. (Paris) **32**, C-1, 1136.
Coqblin, B., and A. Blandin, 1968, Adv. Phys. **17**, 281.
Davis, H. L., 1971, in *Conference Digest No. 3: Rare Earths and Actinides, Durham, 1971* (Institute of Physics, London), p. 126.
Dernier, P. D., E. Bucher, and L. D. Longinotti, 1975, J. Solid State Chem. **15**, 203.
Falicov, L. M., and J. C. Kimball, 1969, Phys. Rev. Lett. **22**, 997.
Freeouf, J. L., D. E. Eastman, W. D. Grobman, F. Holtzberg, and J. B. Torrance, 1974, Phys. Rev. Lett. **33**, 161.
Gardner, W. E., J. Penfold, T. F. Smith, and I. R. Harris, 1972, J. Phys. C **2**, 133.
Gschneidner, K. A., Jr., 1961, *Rare Earth Alloys* (Van Nostrand, Princeton).
Gschneidner, K. A., Jr., R. O. Elliott, and R. R. McDonald, 1962, J. Phys. Chem. Solids **23**, 555, 1191.
Guentherodt, G., and F. Holtzberg, 1975 (to be published).
Havinga, E. E., K. S. J. Buschov, and H. J. van Daal, 1973, Solid State Commun. **13**, 621.
Heine, V., and C. M. Varma, 1974 (unpublished).
Hirst, L. L., 1970, Phys. Kondens Mater **11**, 255.
Hirst, L. L., 1974, J. Phys. Chem. Solids **35**, 1285.
Holtzberg, F., and J. B. Torrance, 1971, in *Proceedings of the 17th Annual Conference on Magnetism and Magnetic Materials*, Chicago, 1971 (AIP Conf. Proc. No. 5), Part 2, p. 860.
Hubbard, J., 1963, Proc. R. Soc. Lond. A **276**, 238.
Hubbard, J., 1964, Proc. R. Soc. Lond. A **277**, 237.
Jayaraman, A., V. Narayanamurti, E. Bucher, and R. G. Maines, 1970, Phys. Rev. Lett. **25**, 1430.
Jayaraman, A., E. Bucher, P. D. Dernier, and L. D. Longinotti, 1973, Phys. Rev. Lett. **31**, 700.
Jayaraman, A., A. K. Singh, A. Chatterjee, and S. Usha Deri, 1974, Phys. Rev. B **9**, 2513.
Jayaraman, A., P. D. Dernier, and L. D. Longinotti, 1975a, Phys. Rev. B **11**, 2783.
Jayaraman, A., P. D. Dernier, and L. D. Longinotti, 1975b, High Temperatures-High Pressures **7**, 1.
Jonker, G. H., and J. H. Van Santen, 1950, Physica **16**, 337.
Kaldis, E., and P. Wachter, 1972, Solid State Commun. **11**, 907.
Khomskii, D. I., and A. N. Kocharjan, 1975, preprint and JETP (to be published).
Lawrence, J. M., M. C. Crofts, and R. D. Parks, 1975, Phys. Rev. Lett. **35**, 289.
Maple, M. B., 1973, in *Magnetism*, edited by H. Suhl (Aca-

---

[1] A more recent experiment [Batlogg *et al.* (1976), Physics Letters, to be published] does not agree with the results of Ward *et al.*

demic, New York), Vol. V, p. 289.
Maple, M. B., and D. Wohleben, 1971, Phys. Rev. Lett. **27**, 511.
Maple, M. B., and D. Wohleben, 1973, in *Proceedings of the 19th Annual Conference on Magnetism and Magnetic Materials,* Boston, 1973 (AIP Conf. Proc. No. 18), Part 1, p. 447.
Melcher, R. L., G. Guntherodt, T. Penney, and F. Holtzberg, 1975, in *Proceedings of the IEEE Symposium on Ultrasonics* (Los Angeles).
Mott, N. F., 1974, Phil. Mag. **30**, 403.
Nagaoka, Y., 1965, Phys. Rev. A **138**, 1112.
Narayanamurti, V., A. Jayaraman, and E. Bucher, 1974, Phys. Rev. **9**, 2521.
Nathan, M. I., F. Holtzberg, J. E. Smith, Jr., J. B. Torrance, and J. C. Tsang, 1975, Phys. Rev. Lett. **34**, 467.
Nickerson, J. C., R. M. White, K. N. Lee, R. Bachman, T. H. Geballe, and G. W. Hull, Jr., 1971, Phys. Rev. **3**, 2030.
Nozières, P., 1975, J. Low Temp. Phys. **17**, 31.
Penney, T., and F. Holtzberg, 1975, Phys. Rev. Lett. **34**, 322.
Pines, D., 1956, Can. J. Phys. **34**, 1379.
Pollak, R. A., F. Holtzberg, J. L. Freeouf, and D. Eastman, 1974, Phys. Rev. Lett. **33**, 820.
Ramirez, R., L. M. Falicov, and J. C. Kimball, 1970, Phys. Rev. B **2**, 3383.
Shapiro, S. M., R. J. Bigeneau, and E. Bucher, 1975, Phys. Rev. Lett. **34**, 470.
Sinha, S. K., and C. M. Varma, 1975 (unpublished).
Tao, L. J., and F. Holtzberg, 1975, Phys. Rev. B **11**, 3842.
Tonkov, E. Yu., and I. L. Aptekar, 1974, Fiz. Tverd. Tela **16**, 1507 [Sov. Phys.—Solid State **16**, 972 (1974)].
Tsuchida, T., and W. E. Wallace, 1965, J. Chem. Phys. **43**, 3811.
van Daal, H. J., K. H. J. Buschow, P. B. van Aken, and M. H. van Marren, 1975, Phys. Rev. Lett. **34**, 1457.
Van Vleck, J. H., 1953, Rev. Mod. Phys. **25**, 220.
Varma, C. M., 1975, Bull. Am. Phys. Soc. **20**, 395.
Varma, C. M., and V. Heine, 1975, Phys. Rev. **11**, 4763.
Varma, C. M., Y. Yafet, and R. L. Cohen, 1975, Bull. Am. Phys. Soc. **20**, 321.
Varma, C. M., and Y. Yafet, 1976, Phys. Rev. (in press).
Wachter, P., 1969, Solid State Commun. **7**, 693.
Walsh, W. M., Jr., L. W. Rupp, Jr., E. Bucher, and L. D. Longinotti, 1974, in *Proceedings of the 19th Annual Conference on Magnetism and Magnetic Materials,* Boston, 1973 (AIP Conf. Proc. No. 18), p. 535.
Ward, R. W., B. P. Clayman, and T. M. Rice, 1975, Solid State Commun. (in press).
Wilson, K. G., 1974, Rev. Mod. Phys. **47**, 773.
Wohleben, D. K., and B. R. Coles, 1973, in *Magnetism,* edited by H. Suhl (Academic, New York), Vol. V, p. 3.